UCRL-16607

University of California

Ernest O. Lawrence Radiation Laboratory

MASS TRANSFER AND POLARIZATION AT A ROTATING DISK ELECTRODE

TWO-WEEK LOAN COPY

This is a Library Circulating Copy
which may be borrowed for two weeks.
For a personal retention copy, call
Tech. Info. Division, Ext. 5545

Berkeley, California

DISCLAIMER

This document was prepared as an account of work sponsored by the United States Government. While this document is believed to contain correct information, neither the United States Government nor any agency thereof, nor the Regents of the University of California, nor any of their employees, makes any warranty, express or implied, or assumes any legal responsibility for the accuracy, completeness, or usefulness of any information, apparatus, product, or process disclosed, or represents that its use would not infringe privately owned rights. Reference herein to any specific commercial product, process, or service by its trade name, trademark, manufacturer, or otherwise, does not necessarily constitute or imply its endorsement, recommendation, or favoring by the United States Government or any agency thereof, or the Regents of the University of California. The views and opinions of authors expressed herein do not necessarily state or reflect those of the United States Government or any agency thereof or the Regents of the University of California.

UCRL-16607

UNIVERSITY OF CALIFORNIA

Lawrence Radiation Laboratory
Berkeley, California

AEC Contract No. W-7405-eng.48

4820

MASS TRANSFER AND POLARIZATION AT A ROTATING DISK ELECTRODE

Limin Hsueh

(M.S. Thesis)

January 1966

CONTENTS

		Page No.
Abstract		1
I.	Introduction	2
II.	Theory of the Rotating Disk Electrode	3
	§2-1 Fluid Flow	3
	§2-2 Mass Transfer	10
	§2-3 Limiting Current Density	12
	§2-4 Numerical Solution Method	13
III.	Polarization at a Rotating Disk Electrode	16
	§3-1 Concentration Overpotential	25
	§3-2 Activation Overpotential	28
	§3-3 Resistance Overpotential	29
IV.	Experimental Work	33
	§4-1 Design and Description of Electrodes	33
	§4-2 The Position of the Reference Electrode	36
	§4-3 Surface Treatment of Electrode	37
	§4-4 The Electrical Circuit	40
	§4-5 Experimental Procedure	43
V.	Results	44
VI.	Summary and Conclusions	52
Acknowledgments		56
Appendices		57
	Appendix A Some Basic Relations for Binary Electrolytes	57
	Appendix B Computer Program	58
Nomenclature		62
Literature Cited		65

MASS TRANSFER AND POLARIZATION AT A ROTATING DISK ELECTRODE

Limin Hsueh
Inorganic Materials Research Division,
Lawrence Radiation Laboratory, and
Department of Chemical Engineering
University of California, Berkeley

ABSTRACT

The rotating disk electrode method is used to study mass transfer and polarization during metal deposition from a binary electrolytic solution at high concentrations. The effects of variation of physical properties in the diffusion layer and of a non-zero interfacial velocity due to the high mass-transfer rate have been taken into consideration in determining the velocity and concentration profiles. The results are used to evaluate the limiting current density and the concentration polarization.

A rigorous way to separate the total overpotential as the sum of concentration overpotential, activation overpotential and resistance overpotential in a concentrated solution is given. The proper choice of the location of the reference electrode and the surface treatment of electrodes for a metal deposition reaction are discussed.

For the limiting current density measurement in a low conductivity electrolyte, the method of "limiting speed" is introduced so that the resistance overpotential can be held constant. The experimental results of limiting current divided by the square root of the rotating speed, $i_{lim}/\sqrt{\Omega}$, are found to agree well with the theoretically predicted values at high concentrations.

I. INTRODUCTION

The rotating disk electrode has been widely used as a tool for studying electrode processes and mass transfer because the velocity and concentration profiles can be predicted theoretically and the strong forced convection eliminates the effects of natural convection. Two branches of work have been done on this field:

i. to study mass transfer processes by means of the limiting current density or to obtain the diffusion coefficient as a function of concentration.

ii. to study electrode kinetics by means of the polarization curve, so as to obtain the kinetic parameters of the reaction as functions of concentrations, or as they are modified by additional agents.

For the first part, the theory of concentration polarization was developed in 1942 by Levich[1]. The original theory of Levich involved the assumptions of constant physical properties throughout the diffusion layer and a zero interfacial velocity at the surface of the disk. In order to meet these assumptions, most experimental work has been done at relatively low concentrations (e.g., 10^{-5} to 10^{-3}M).

For the second branch, the main interest centered on activation polarization. In order to keep the uncertain value of ohmic resistance as low as possible, most experimental work involved high concentrations (e.g., 0.1 to 1 M), with excess supporting electrolyte. Generally the current density was low, far from the limiting current density.

For the case of constant physical properties of the electrolytic solution the (hydrodynamic) theory of the rotating disk electrode and its applications are given in the book of Levich[2] and a review paper

by Riddiford[3]. The transient effect of hydrodynamics and mass transfer at a rotating disk were studied by Olander[4], Hale[5], and Filinovskii and Kiryanov[6].

Recently, the variation of physical properties and non-zero interfacial mass transfer velocity have been taken into consideration for a binary, concentrated electrolyte. Both the velocity profile and the concentration profile for the rotating disk electrode have been solved by Newman and Hsueh[7]. Therefore, the primary aim of this work is to study the mass transfer rate by a limiting current technique for comparison with the theoretical results where the variation of physical properties in the diffusion layer was taken into consideration. The experiments were carried out with concentrated solutions without any supporting electrolyte.

Since the theoretical analysis involves solutions of a single salt, a metal deposition reaction in the system of copper-copper sulfate was chosen for this investigation, in apite of the fact that the metal deposition reaction has the following experimental difficulties compared with a redox reaction:

i. the electrode surface cannot remain unaltered;

ii. it takes a longer time to reach the steady state electrode potential, as was pointed out by Brown and Thirsk[8].

II. THEORY OF THE ROTATING DISK ELECTRODE

§2-1 Fluid Flow

The general analytic approach to the influence of physical property variation on the velocity and concentration profiles was first solved by Olander[9] in 1962 for steady, laminar flow at high Schmidt numbers.

In his paper, two parameters ϵ_D and ϵ_ρ were defined as follows:

$$\epsilon_D = -(\omega_{zero} - \omega_\infty)\frac{1}{D}\frac{dD}{d\omega_s} = \ln\left(\frac{D_\infty}{D_{zero}}\right)$$

$$\epsilon_\rho = -(\omega_{zero} - \omega_\infty)\frac{1}{\rho}\frac{d\rho}{d\omega_s} = \ln\left(\frac{\rho_\infty}{\rho_{zero}}\right)$$

where ω_s mass fraction of salt

D diffusion coefficient

ρ density of solution

subscript ∞ in the bulk of solution

zero at interface of electrode.

With the assumption that the density and diffusivity vary exponentially with mass fraction over the concentration range of interest, i.e., both ϵ_D and ϵ_ρ are independent of composition, the rate of mass transfer in terms of the Nusselt number was solved by a perturbation method.

Without involving any limitation on how the physical properties vary with concentration, Newman and Hsueh[7] have obtained numerical solutions of the velocity and concentration profiles for a binary, concentration electrolyte. We summarize here their method and results.

The analysis applies to a disk which provides a uniformly accessible surface and rotates horizontally about an axis through its center perpendicular to the plane of the disk at a constant angular speed Ω in a Newtonian fluid.

From an experimental viewpoint we must make the further assumptions that:

i. in order to maintain steady, laminar flow, the Reynolds number should not exceed 2×10^5. The Reynolds number for a rotating disk is defined as $\frac{r^2\Omega}{\nu}$ where r is the radius of disk, Ω is the angular velocity

of disk (radians per second) and ν is the kinematic viscosity of the fluid.

ii. the effect of natural convection may be ignored, since the solution is strongly stirred by the disk.

iii. there are no bounding surfaces which may affect the velocity and concentration profile. By bounding surface, we mean the wall of the vessel, an air-solution interface, or any other experimental equipment, such as a thermometer, or a reference electrode.

iv. the edge effects can be neglected both in the mass transfer and in the hydrodynamic analysis.

For the velocity profile, the equation of motion has to be solved; for steady state it reads

$$\rho \underline{v} \cdot \nabla \underline{v} = - \nabla p - \nabla \cdot \underline{\underline{\tau}} + \rho \underline{g} \tag{2-1}$$

where $\underline{\underline{\tau}}$ is the stress tensor which for a Newtonian fluid reads in rectangular coördinates

$$\tau_{ij} = - \mu \left[\frac{\partial v_j}{\partial x_i} + \frac{\partial v_i}{\partial x_j} \right] + \frac{2}{3} \mu \, (\nabla \cdot \underline{v}) \, \delta_{ij} \tag{2-2}$$

where δ_{ij} is the Kronecker delta

$$\delta_{ij} = 1 \quad \text{if} \quad i = j$$

$$\delta_{ij} = 0 \quad \text{if} \quad i \neq j \, .$$

The equation of motion must be solved together with the equation of continuity

$$\nabla \cdot (\rho \underline{v}) = 0 \, . \tag{2-3}$$

Because of the nature of the rotating disk, it is convenient to choose cylindrical coördinates r, θ and z, where r is the radial distance from the axis of roation, θ is the circumferential angle of rotation, and z is the normal distance from the disk. The corresponding velocity

components are v_r, v_θ and v_z, respectively.

By axial symmetry, all three velocity components are independent of θ. Furthermore, in solving for the velocity profile of the system, the most important feature which provides the major simplification from a set of partial differential equations to ordinary differential equations is that the z-component of velocity can be assumed to be a function of the perpendicular distance from the disk surface only. It is independent to the radial distance. Physically, this means that v_z brings fresh reacting ions to the electrode surface at a uniform rate over the whole disk.

It should be emphasized that the vector sum of v_r, v_θ and v_z does not have to be identical for the same distance from the disk, because of the dependence of v_r and v_θ on r.

The above assumptions are summarized as follows

$$v_r = v_r(r,z)$$
$$v_\theta = v_\theta(r,z)$$
$$v_z = v_z(z)$$
$$p = p(z).$$

Since under these conditions v_z is the only velocity component which can affect the concentration in the boundary layer, one may conclude that the concentration near the disk is a function of z only. Furthermore, all the physical properties, such as density, viscosity, diffusivity, electric conductivity, and transference number of an electrolyte depend on concentration only at a constant temperature. Therefore all of the physical properties are assumed to vary in the z-direction only.

The components of the equation of motion, Equation (2-1), are given

in cylindrical coördinates in Bird, Steward and Lightfoot[10a].

$$\left.\begin{aligned}
\rho\left(v_r\frac{\partial v_r}{\partial r} - \frac{v_\theta^2}{r} + v_z\frac{\partial v_r}{\partial z}\right) &= -\frac{1}{r}\frac{\partial}{\partial r}(r\,\tau_{rr}) - \frac{\tau_{\theta\theta}}{r} + \frac{\partial \tau_{rz}}{\partial z}\,,\\
\rho\left(v_r\frac{\partial v_\theta}{\partial r} + \frac{v_r v_\theta}{r} + v_z\frac{\partial v_\theta}{\partial z}\right) &= -\frac{1}{r^2}\frac{\partial}{\partial r}(r^2\tau_{r\theta}) + \frac{\partial \tau_{\theta z}}{\partial z}\,,\\
\rho v_z\frac{dv_z}{dz} &= -\frac{dp}{dz} - \frac{1}{r}\frac{\partial}{\partial r}(r\,\tau_{rz}) + \frac{\partial \tau_{rz}}{\partial z} + \rho g_z\,,
\end{aligned}\right\}\quad(2\text{-}4)$$

where the nine components of the stress tensor in cylindrical coördinates are[10b]

$$\left.\begin{aligned}
\tau_{rr} &= -\mu\left[2\frac{\partial v_r}{\partial r} - \frac{2}{3}\left(\frac{1}{r}\frac{\partial}{\partial r}(r\,v_r) + \frac{dv_z}{dz}\right)\right],\\
\tau_{\theta\theta} &= -\mu\left[2\frac{v_r}{r} - \frac{2}{3}\left(\frac{1}{r}\frac{\partial}{\partial r}(r\,v_r) + \frac{dv_z}{dz}\right)\right],\\
\tau_{zz} &= -\mu\left[2\frac{dv_z}{dz} - \frac{2}{3}\left(\frac{1}{r}\frac{\partial}{\partial r}(r\,v_r) + \frac{dv_z}{dz}\right)\right],\\
\tau_{r\theta} = \tau_{\theta r} &= -\mu\left[r\frac{\partial}{\partial r}\left(\frac{v_\theta}{r}\right)\right],\\
\tau_{\theta z} = \tau_{z\theta} &= -\mu\left[\frac{\partial v_\theta}{\theta z}\right],\\
\tau_{zr} = \tau_{rz} &= -\mu\left[\frac{\partial v_r}{\partial z}\right].
\end{aligned}\right\}\quad(2\text{-}5)$$

The equation of continuity becomes

$$\frac{1}{r}\frac{\partial}{\partial r}(r\,v_r) + \frac{dv_z}{dz} = -\frac{v_z}{\rho}\frac{d\rho}{dz}\,. \qquad (2\text{-}6)$$

Since we are interested in a concentrated, binary electrolyte, the mass transfer rate at the surface is very high, and the interfacial velocity will no longer be zero. If a metal deposition reaction is being considered, the cation is the only substance which carries current to the electrode surface. In other words, the flux of anions N_{-z} and

the flux of the solvent N_{oz} are both zero at the surface.

$$N_{oz} = N_{-z} = 0 \quad \text{at } z = 0$$
$$N_{+z} = \frac{i_z}{Fz_+} \quad \text{at } z = 0 \tag{2-7}$$

where i_z is the current density normal to the electrode,

F is Faraday's constant.

From here on, the subscript "+" refers to cations or cathodic, "-" refers to anions or anodic, and "o" refers to the solvent.

The mass average velocity is defined as

$$\underline{v} = \frac{\sum_i \rho_i \underline{v}_i}{\sum_i \rho_i} . \tag{2-8}$$

If the relation between mass flux and molar flux is used

$$n_i = \rho_i v_i = \underline{N}_i M_i$$

together with Equations (2-7) and (2-8), one obtains

$$v_z = \frac{i_z M_+}{\rho F z_+} \tag{2-9}$$

where M is molecular weight.

This is a major difference in the boundary condition compared with von Karman's solution[11] where the Navier-Stokes equation was solved with the boundary condition $v_z = 0$ at $z = 0$.

In order to give an idea of the order of magnitude of v_z at z=0 when a rotating disk electrode is operated at limiting current density, i.e., the maximum rate of mass transfer, we present an example. If a disk electrode is rotated at a speed of 300 r.p.m. in 0.1 M copper sulfate solution at 25°C, the limiting current density is 79mA/cm^2, and

v_z equals 2.60×10^{-5} cm/sec at the disk, compared with $v_z = 4.7 \times 10^{-1}$ cm/sec far from disk.

At the interface, the other two velocity components are

$$v_r = 0, \qquad v_\theta = r\Omega \qquad \text{at } z = 0 .$$

As z increases, v_r and v_θ must tend to die away, i.e.,

$$v_r = 0, \qquad v_\theta = 0 \qquad \text{at } z = \infty .$$

A dimensionless distance ξ, and dimensionless velocities F, G, and H are defined as follows:

$$\xi = z\sqrt{\frac{\Omega}{\nu_\infty}} \tag{2-10}$$

$$\left.\begin{aligned} v_r &= r\Omega F(\xi) \\ v_\theta &= r\Omega G(\xi) \\ v_z &= \sqrt{\Omega\nu_\infty}\, H(\xi) \end{aligned}\right\} \tag{2-11}$$

$$p = \mu_\infty \Omega P(\xi) + g_z \int_0^z \rho dz . \tag{2-12}$$

These definitions assume the same dependence for v_r and v_θ as assumed by von Karman.[11] Now the nine components of the stress tensor become

$$\left.\begin{aligned} \tau_{rr} = \tau_{\theta\theta} &= -\frac{2}{3}\mu\Omega(F-H') \\ \tau_{zz} &= \frac{4}{3}\mu^\circ(F-H') \\ \tau_{r\theta} = \tau_{\theta r} &= 0 \\ \tau_{\theta z} = \tau_{z\theta} &= -\mu r\Omega G'\sqrt{\frac{\Omega}{\nu_\infty}} \\ \tau_{zr} = \tau_{rz} &= -\mu r\Omega F'\sqrt{\frac{\Omega}{\nu_\infty}} \end{aligned}\right\} \tag{2-13}$$

and the equation of motion becomes:

$$\left.\begin{aligned} F^2 - G^2 + HF' &= \frac{\rho_\infty}{\rho}\frac{d}{d\xi}\left(\frac{\mu}{\mu_\infty}F'\right) \\ 2FG + HG' &= \frac{\rho_\infty}{\rho}\frac{d}{d\xi}\left(\frac{\mu}{\mu_\infty}G'\right) \\ \frac{\rho}{\rho_\infty}HH' + P' &= \frac{4}{3}\frac{d}{d\xi}\left[\frac{\mu}{\mu_\infty}(H'-F)\right] + \frac{2\mu}{\mu_\infty}F' \end{aligned}\right\} \quad (2\text{-}14)$$

and the equation of continuity becomes

$$2F + H' = -H\frac{1}{\rho}\frac{d\rho}{d\xi} \quad (2\text{-}15)$$

where primes denote differentiation with respect to ξ. The boundary conditions become

$$\xi = 0 \qquad F(0) = 0 \qquad G(0) = 1$$

$$\xi = \infty \qquad F(\infty) = 0 \qquad G(\infty) = 0.$$

Since the variation of pressure due to the hydraulic head is very small and the variation of the fluid properties due to pressure is negligible, it is not necessary to solve z-component of the equation of motion (2-14), the only equation where the variation of pressure has been involved.

§2-2 Mass Transfer

The mechanism of transfer of cations from the bulk of the solution to the surface of the cathode consists, essentially, of three processes: molecular diffusion, migration, and convection. At steady state, the sum of the rate of these three processes is balanced by the rate of discharging at the electrode surface.

The flux of cations can be expressed as[12]

$$N_+ = -\nu_+\frac{D\rho}{M_s}\nabla\omega_s + \frac{\underline{i}t_+}{Fz_+} + C_+\underline{v} \quad (2\text{-}16)$$

where t_+ cation transference number with respect to mass average velocity

M_s molecular weight of salt

ν_+ number of cations produced by dissociation of one molecule of electrolyte.

For consistency with the velocity profile of the previous section, the mass average velocity was chosen as the basis of the flux equation. This is the reason that the mass fraction gradient is used instead of a concentration gradient as the driving force for molecular diffusion.

If a material balance is applied to the cation over a volume element, the equation of continuity reads

$$\frac{\partial C_+}{\partial t} = - \nabla \cdot N_+ \ . \tag{2-17}$$

Inserting Equation (2-16) into Equation (2-17), with use of the basic relations of Equations (A-2), (A-4) and (A-5) for a binary electrolyte (see Appendix A) yields

$$\rho \frac{\partial \omega_s}{\partial t} + \rho \underline{v} \cdot \nabla \omega_s = \nabla \cdot (\rho D \nabla \omega_s) - \frac{M_s \underline{i} \cdot \nabla t_+}{z_+ \nu_+ F} \ . \tag{2-18}$$

As it was assumed in section 2-1 that all physical properties vary in the z direction only, Equation (2-16) can be written

$$N_{+z} = - \nu_+ \frac{D\rho}{M_s} \frac{d\omega_s}{dz} + \frac{i_z t_+}{F z_+} + C_+ v_z \ . \tag{2-19}$$

At steady state, Equation (2-18) becomes

$$\rho v_z \frac{d\omega_s}{dz} + \frac{M_s i_z}{z_+ \nu_+ F} \frac{dt_+}{dz} = \rho D \frac{d^2 \omega_s}{dz^2} + \frac{d\omega_s}{dz} \frac{d}{dz} (\rho D) \ . \tag{2-20}$$

The boundary conditions are

$$\begin{aligned} z &= 0 \qquad \omega_s = \omega_{zero} \\ z &= \infty \qquad \omega_s = \omega_\infty \ . \end{aligned} \tag{2-21}$$

When the dimensionless variables ξ and H which have been defined in Equation (2-10) and (2-11) are introduced into Equation (2-20), it becomes

$$\left(\frac{\rho}{\rho_\infty} H + I \frac{dt_+}{d\omega_s}\right) \frac{d\omega_s}{d\xi} = \frac{d}{d\xi}\left(\frac{\rho D}{\mu_\infty} \frac{d\omega_s}{d\xi}\right) \tag{2-22}$$

where I is a dimensionless current density defined as

$$I = \frac{M_s i_z}{\rho_\infty \nu_+ z_+ F \sqrt{\Omega \nu_\infty}} .$$

It is clear that the current density is proportional to the square root of speed even in a concentrated solution.

Formal integration of Equation (2-22) gives

$$\omega_s = K_1 \int_0^\xi \frac{\mu_\infty}{\rho D} \exp \int_0^\xi \frac{\mu_\infty}{\rho D}\left(\frac{\rho}{\rho_\infty} H + I \frac{dt_+}{d\omega_s}\right) d\xi + K_2$$

where K_1 and K_2 are constants of integration to be determined by the boundary conditions (2-21). Finally, the concentration profile is

$$\frac{\omega_s - \omega_{zero}}{\omega_\infty - \omega_{zero}} = \frac{\int_0^\xi \frac{\mu_\infty}{\rho D} \exp \int_0^\xi \frac{\mu_\infty}{\rho D}\left(\frac{\rho}{\rho_\infty} H + I \frac{dt_+}{d\omega_s}\right) d\xi \, d\xi}{\int_0^\xi \frac{\mu_\infty}{\rho D} \exp \int_0^\xi \frac{\mu_\infty}{\rho D}\left(\frac{\rho}{\rho_\infty} H + I \frac{dt_+}{d\omega_s}\right) d\xi \, d\xi} . \tag{2-23}$$

Because of the non-zero interfacial velocity, the dimensionless current I is further related to the dimensionless axial velocity H by Equation (2-9) in the form

$$H(0) = \frac{\rho_\infty}{\rho} \frac{\nu_+ M_+ I}{M_s} \quad \text{at } \xi = 0 . \tag{2-24}$$

§2-3 Limiting Current Density

The rate of charge transfer at the electrode surface in a metal deposition reaction by passing a current i_z at the cathode is $\frac{i_z}{Fz_+}$.

At steady state, it should be balanced by the rate of mass transfer to the surface by diffusion, migration and convection which has been defined in Equation (2-19):

$$\frac{i_z}{Fz_+} = - \nu_+ \frac{D\rho}{M_s} \frac{d\omega_s}{dz} + \frac{i_z}{Fz_+} t_+ + \frac{\rho}{M_+} \omega_+ v_z \qquad \text{at } z = 0. \tag{2-25}$$

Notice that the convection term is not zero at the surface. Substitution of Equation (2-9) into Equation (2-25) and solving for the current density yields

$$i_z = \frac{\rho D F z_+ \nu_+}{M_s(1-t_+-\omega_+)} \frac{d\omega_s}{dz}\bigg|_{z=0} \tag{2-26}$$

or in dimensionless form

$$I = - \frac{\rho D}{M_\infty(1-t_+-\omega_+)} \frac{d\omega_s}{d\xi}\bigg|_{\xi=0} . \tag{2-27}$$

This relates the current I to the concentration profile at the metal-solution interface, and it also serves as a boundary condition for solving the concentration profile in section 2-2. The limiting current density is obtained from Equation (2-26) by letting the interfacial mass fraction of salt ω be zero

$$\frac{i_{lim}}{\sqrt{\Omega}} = - \frac{\rho D F z_+ \nu_+}{\sqrt{\nu_\infty}\, M_s(1-t_+)} \frac{d\omega_s}{d\xi}\bigg|_{\xi=0} . \tag{2-28}$$

§2-4 Numerical Solution Method

In the previous sections, a set of nonlinear equations were derived that would give the velocity profile at the disk and the concentration profile in the diffusion region. The equations to be solved numerically and their boundary conditions are summarized below

$$\left.\begin{aligned} F^2 - G^2 + HF' &= VF'' + U'F' \\ 2FG + HF &= VG'' + U'G' \end{aligned}\right\} \qquad (2\text{-}14)$$

$$2F + H' = - HR' \qquad (2\text{-}15)$$

$$\frac{d}{d\xi}\left(\frac{\rho D}{\mu_\infty}\omega_s'\right) - \left(\frac{\rho}{\rho_\infty} H + I\frac{dt_+}{d\omega_s}\right)\omega_s' = 0 \qquad (2\text{-}22)$$

where

$$V = \frac{\mu}{\mu_\infty}\frac{\rho_\infty}{\rho}$$

$$U' = \frac{\rho_\infty}{\rho}\frac{d}{d\xi}\left(\frac{\mu}{\mu_\infty}\right)$$

$$R' = \frac{d\ \ln \rho}{d\xi} \ .$$

We have four unknowns, F, G, H, and ω_s to be determined as functions of ξ by these four equations. Since V, U', and R' are related to the concentration, they are not independent variables but are known once the concentration profile has been obtained. The boundary conditions are

$$\begin{aligned} &\text{at } \xi = \infty \quad F = 0 \quad G = 0 \quad \omega = \omega_\infty \\ &\xi = 0 \quad F = 0 \quad G = 1 \quad \omega = \omega_{zero} \end{aligned} \qquad (2\text{-}21)$$

$$H = \frac{\rho_\infty}{\rho}\frac{\nu_+ M_+ I}{M_s} \qquad (2\text{-}24)$$

$$I = \frac{M_s i_z}{\rho_\infty \nu_+ z_+ F\sqrt{\Omega\nu_\infty}} = - \frac{\rho D}{\mu_\infty(1-t_+-M_\infty)}\left.\frac{d\omega}{d\xi}\right|_{\xi=0} \ . \qquad (2\text{-}28)$$

In order to solve equations (2-14) and (2-15), we have to linearize them by assuming each variable, F, G, and H, to be the sum of a main term and a first order correction, i.e.,

$$\begin{aligned} F &= F_o + F_1 \\ G &= G_o + G_1 \\ H &= H_o + H_1 \ . \end{aligned}$$

By substituting F, G, and H into Equation (2-14) and (2-15), neglecting the products of correction terms, and replacing all remaining F_1, G_1, and H_1 by the original functions F, G, and H and F_o, G_o, and H_o, those differential equations become

$$VF'' + (U' - H_o)\,F' - (2F_oF - 2G_oG + F_o'H) = -\,(H_oF_o' + F_o^2 - G_o^2) \qquad (2\text{-}29)$$

$$VG'' + (U' - H_o)\,G' - (2G_oF + 2F_oG + G_o'H) = -\,(H_oG_o' + 2F_oG_o) \qquad (2\text{-}30)$$

$$H' + (2F + R'H) = 0\,. \qquad (2\text{-}31)$$

It is clear that Equations (2-29) and (2-30) are linear in F and G, respectively, now. The next step is to convert them into difference equations so that they can be solved with a computer. With a mesh size of h the first and second central difference quotients for F and G are

$$F' = \frac{F_{j+1} - F_{j-1}}{2h} \qquad F'' = \frac{F_{j+1} - 2F_j + F_{j-1}}{h^2}$$

$$G' = \frac{G_{j+1} - G_{j-1}}{2h} \qquad G'' = \frac{G_{j+1} - 2G_j + G_{j-1}}{h^2}\,.$$

Substitution into Equations (2-29), (2-30) and rearrangement gives

$$\left(\frac{V_j}{h^2} + \frac{U_j' - H_{oj}}{2h}\right)F_{j+1} - 2\left(\frac{V_j}{h^2} + F_{oj}\right)F_j + \left(\frac{V_j}{h^2} - \frac{U_j' - H_{oj}}{2h}\right)F_{j-1}$$
$$- F_{oj}'H_j + 2G_{oj}F_j = -\,H_{oj}F_{oj}' - F_{oj}^2 + G_{oj}^2\,. \qquad (2\text{-}32)$$

$$\left(\frac{V_j}{h^2} + \frac{U_j' - H_{oj}}{2h}\right)G_{j+1} - 2\left(\frac{V_j}{h^2} + F_{oj}\right)G_j + \left(\frac{V_j}{h^2} - \frac{U_j' - H_{oj}}{2h}\right)G_{j-1}$$
$$- G_{oj}'H_j - 2G_{oj}F_j = -\,H_{oj}G_{oj}' - 2F_{oj}G_{oj}\,. \qquad (2\text{-}33)$$

Since only the first derivative is involved in Equation (2-31), the central difference quotient would cause the coefficient of H at the mesh point j to be zero if $R' = 0$, i.e., if density is constant. In view of this, the backward difference quotient was chosen and all numerical values were evaluated half-way between the mesh point j and j-1:

$$H' = \frac{1}{h}\,(H_j - H_{j-1}) \qquad F = \frac{1}{2}\,(F_j + F_{j-1})$$

$$R'H = \frac{1}{2}\,(R_j'H_j + R_{j-1}'H_{j-1})\,.$$

The difference equation for Equation (2-31) is

$$(\tfrac{1}{2}R'_j h + 1)\, H_j + \tfrac{1}{2}(R'_{j-1}\, h - 1)\, H_{j-1} + F_j h + F_{j-1}\, h = 0 \qquad (2\text{-}34)$$

The finite difference equations were solved on a high speed computer by solving the coupled tri-diagonal matrices, with a mean size of 0.01. Based on the asymptotic solution of the fluid mechanics for large ξ[13], the boundary conditions at infinity were replaced by those at a finite distance, say $\xi = 10$, which is far beyond the hydrodynamic and diffusion boundary layers.

As for the concentration profile, Equation (2-22) has been solved analytically to yield the form of Equation (2-23). The trapezoidal rule was used for numerical integration of the latter equation. The upper limit of integration was replaced by the last mesh point.

Data for the physical properties of copper sulfate solutions at 25°C were collected from the literature[32-47]. Most of these were fitted by linear regression to finite power series in the mass fraction of copper sulfate. The graphs of the data and their equations are shown in Figures 2-1 to 2-5.

The calculated velocity profile for 0.02M and 0.5M copper sulfate solution are shown in Figure 2-6 and Figure 2-7. The velocity profile for 0.02M is very close to von Kármán's solution[11], which may serve as a reference for the purpose of comparison.

III. POLARIZATION AT A ROTATING DISK ELECTRODE

A great many studies have been made on the subject of the kinetics of electrode processes. The main purpose is to study the mechanisms of an electrode reaction and to relate the current density to the total overpotential measured. Vetter[14] presented an extensive survey of this

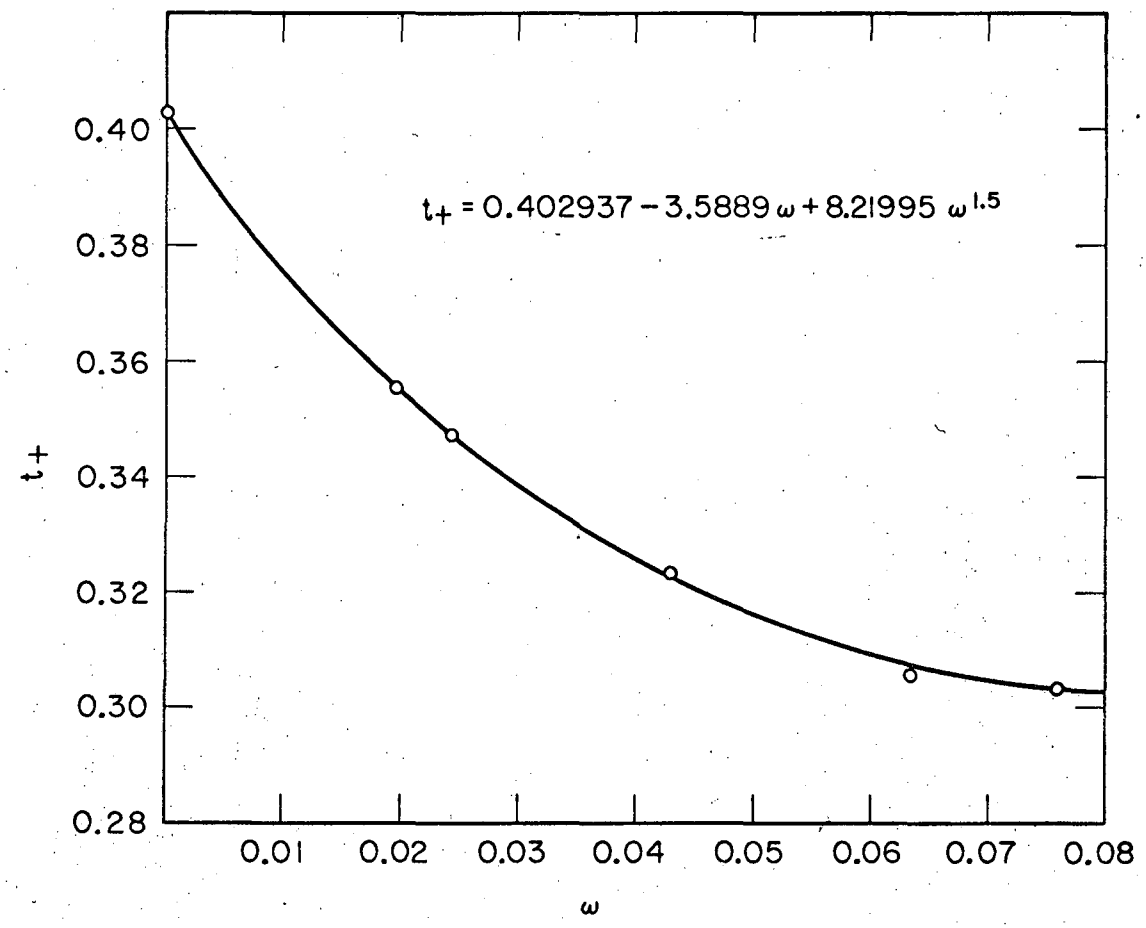

Figure 2-1. Transference number of $CuSO_4$ solutions at 25°C.
○ Fritz and Fuget[32]

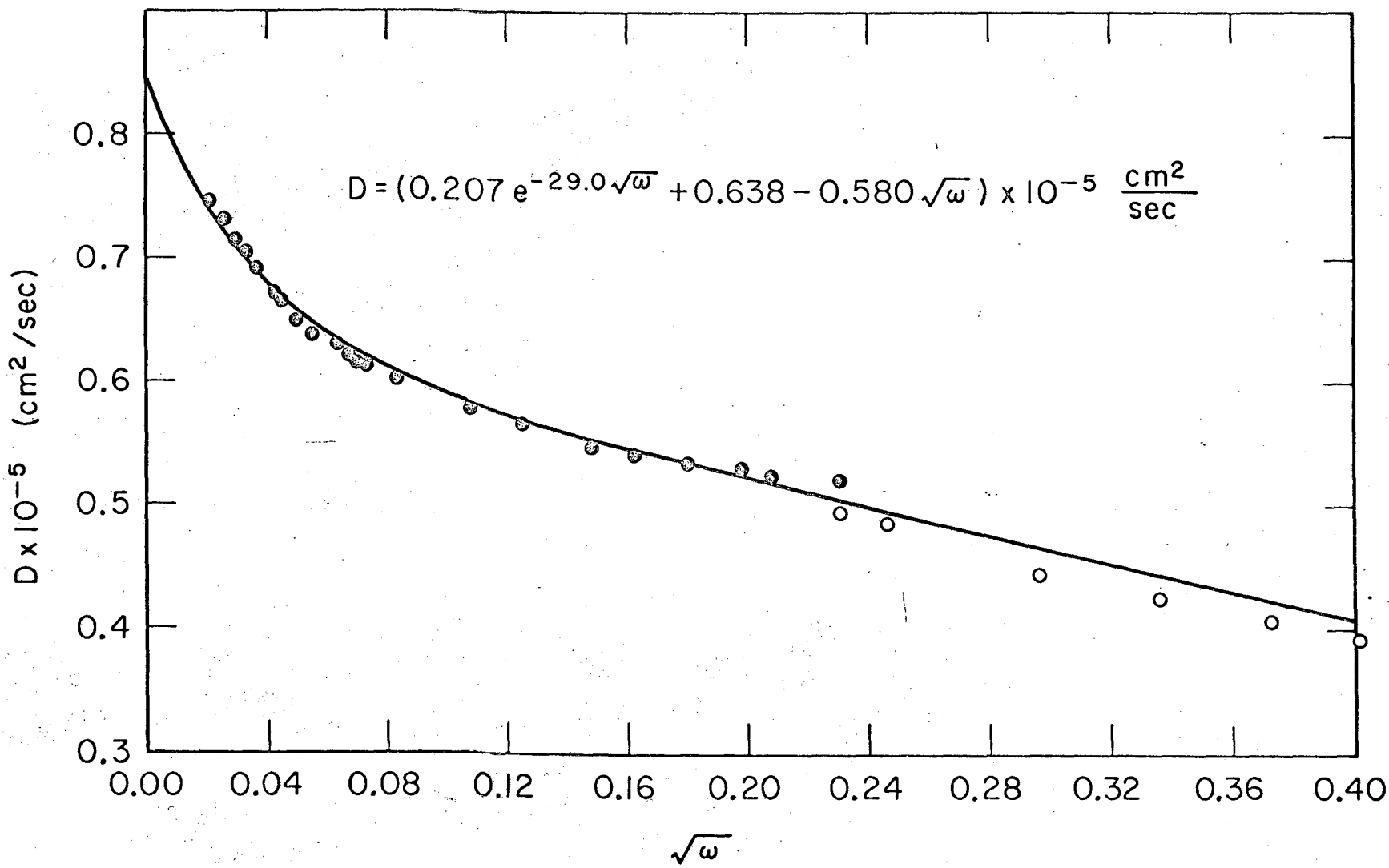

Figure 2-2. Diffusion coefficient of $CuSO_4$ solutions at 25°C.
● Eversole, Kindsvater and Peterson[33]
○ Emanuel and Olander[34]

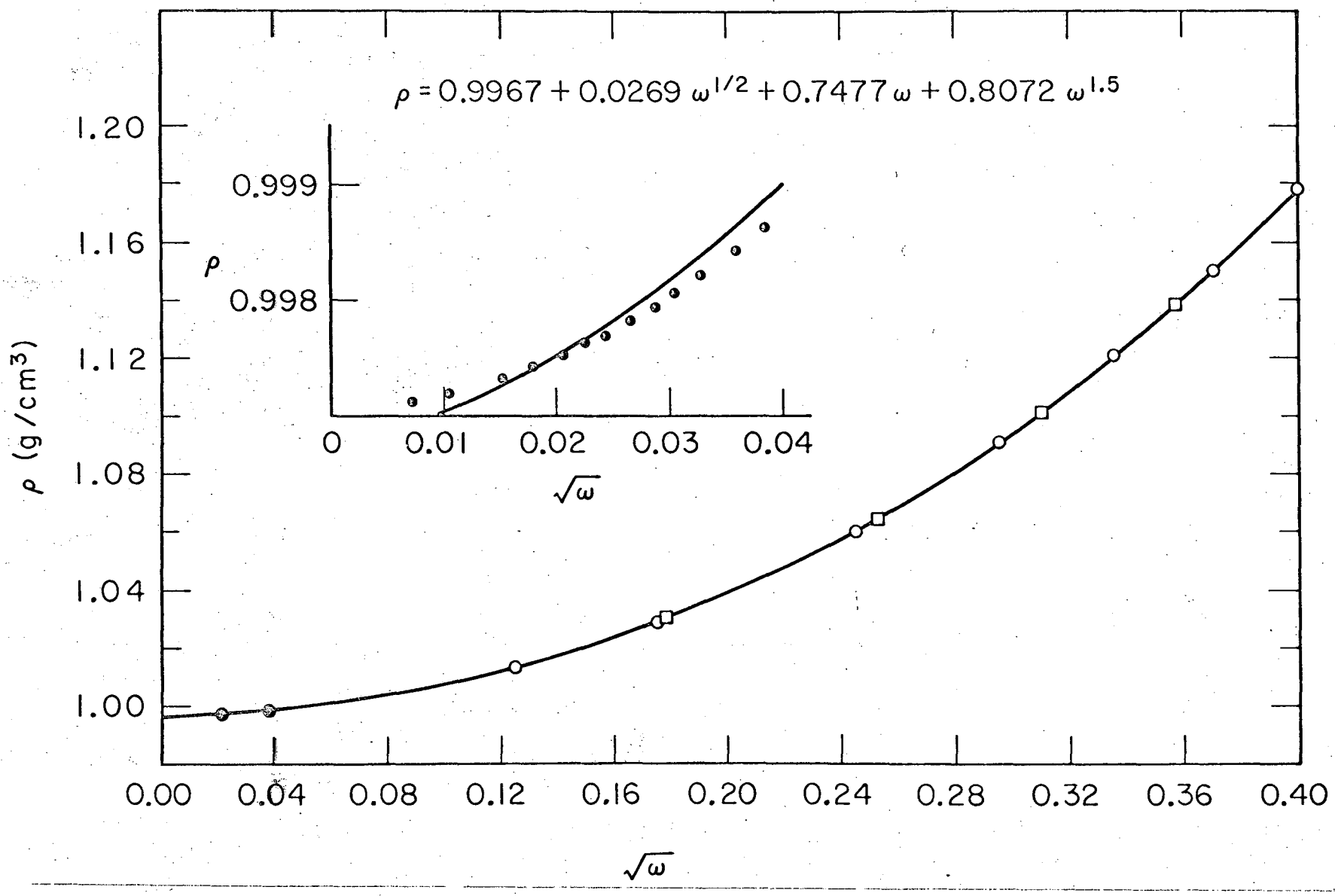

Figure 2-3. Density of $CuSO_4$ solutions at 25°C.
○ Pearce and Pumplin[35]
● Asmus[36]
□ Holler and Peffer[37]

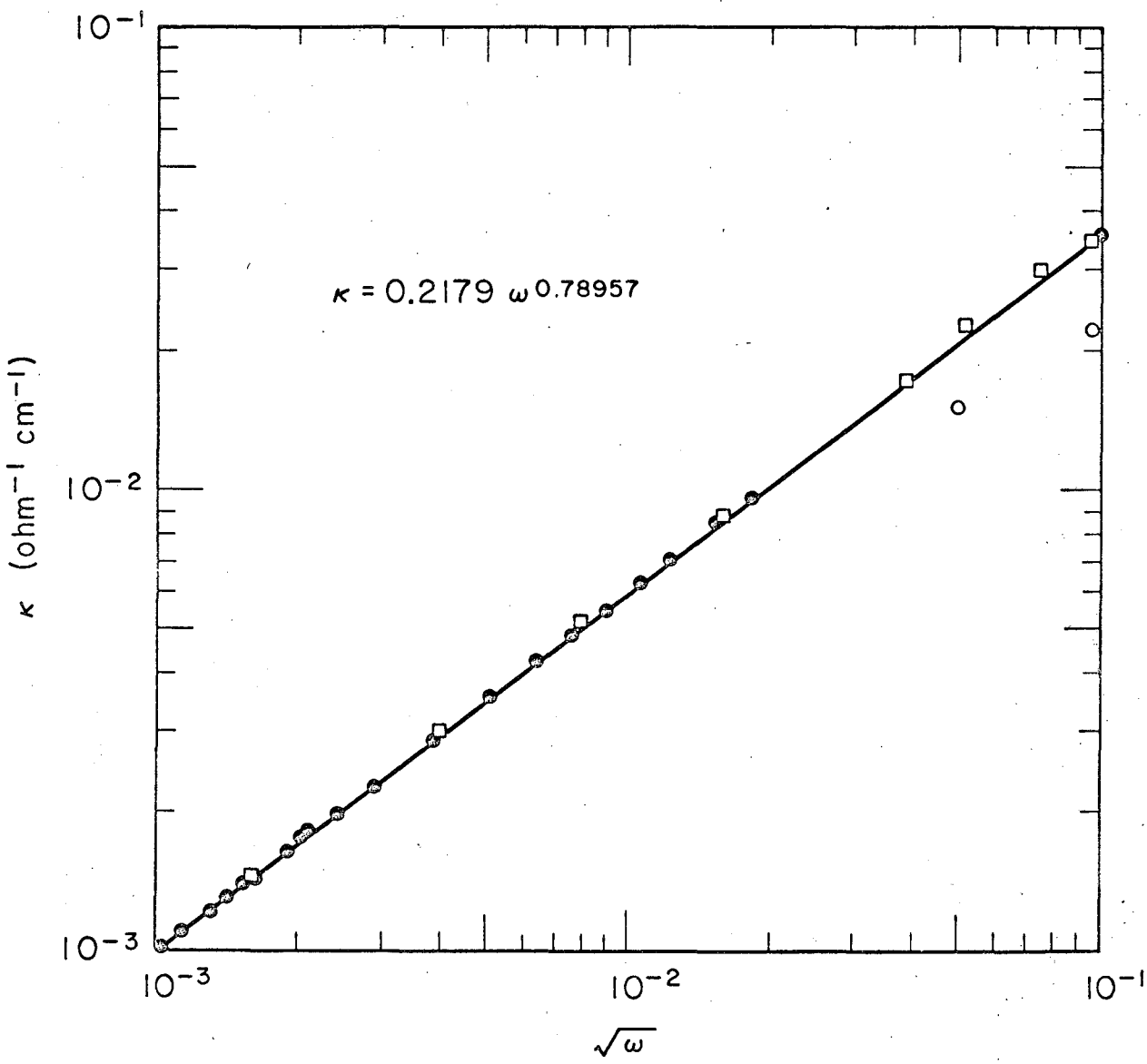

Figure 2-4. Specific conductivity of $CuSO_4$ solutions at 25°C.
● Owen and Gurry[38]
◐ Richardson and Taylor[39]
□ Fedoroff[40]

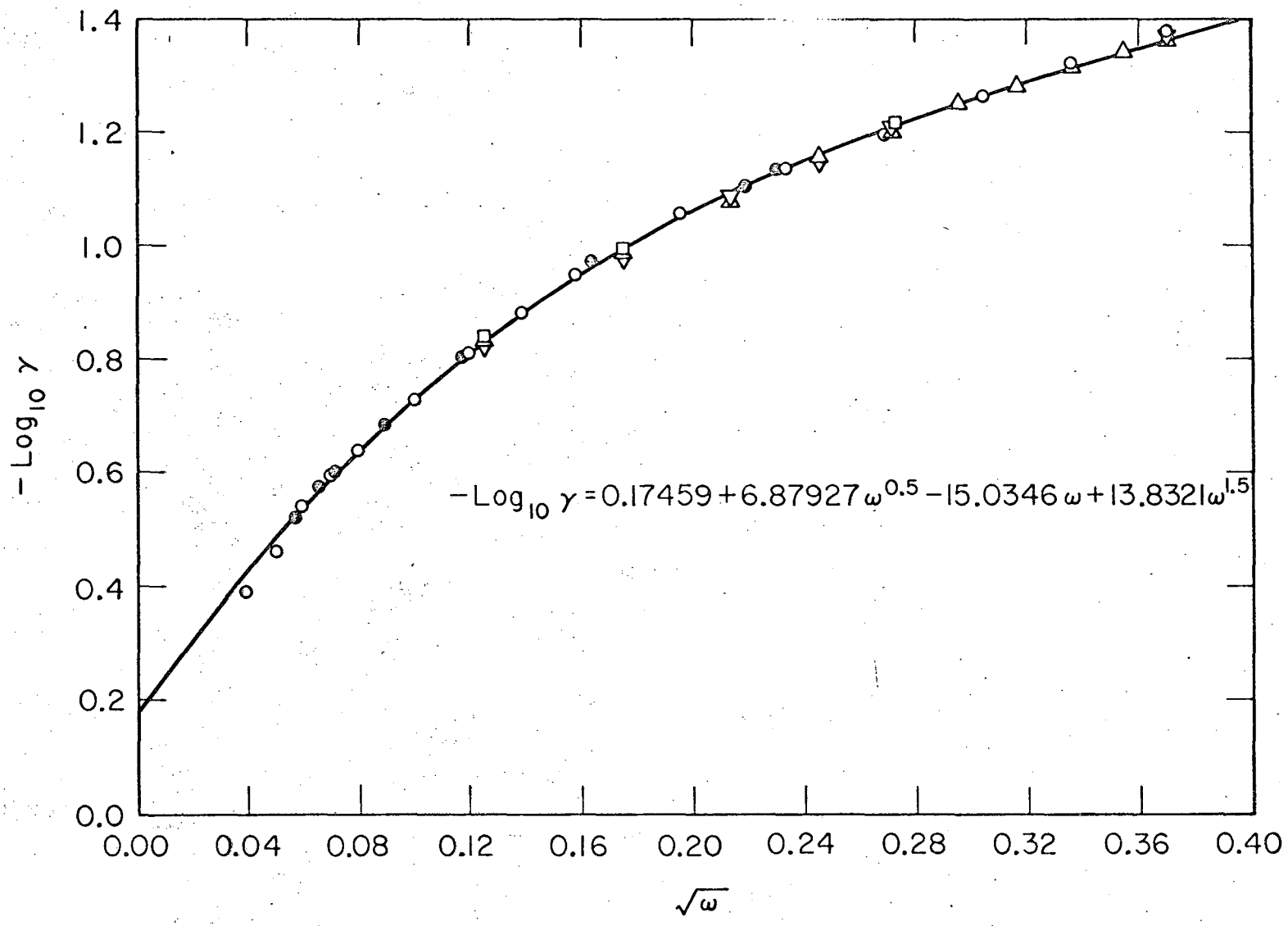

Figure 2-5. Mean activity coefficient of $CuSO_4$ solutions at 25°C.
□ Nielsen and Brown[41] Adjusted ▽ Robinson and Jones[42] Adjusted
● Wetmore and Gordon[43] ○ Wetmore and Gordon Smoothed
△ Robinson and Stokes[44]

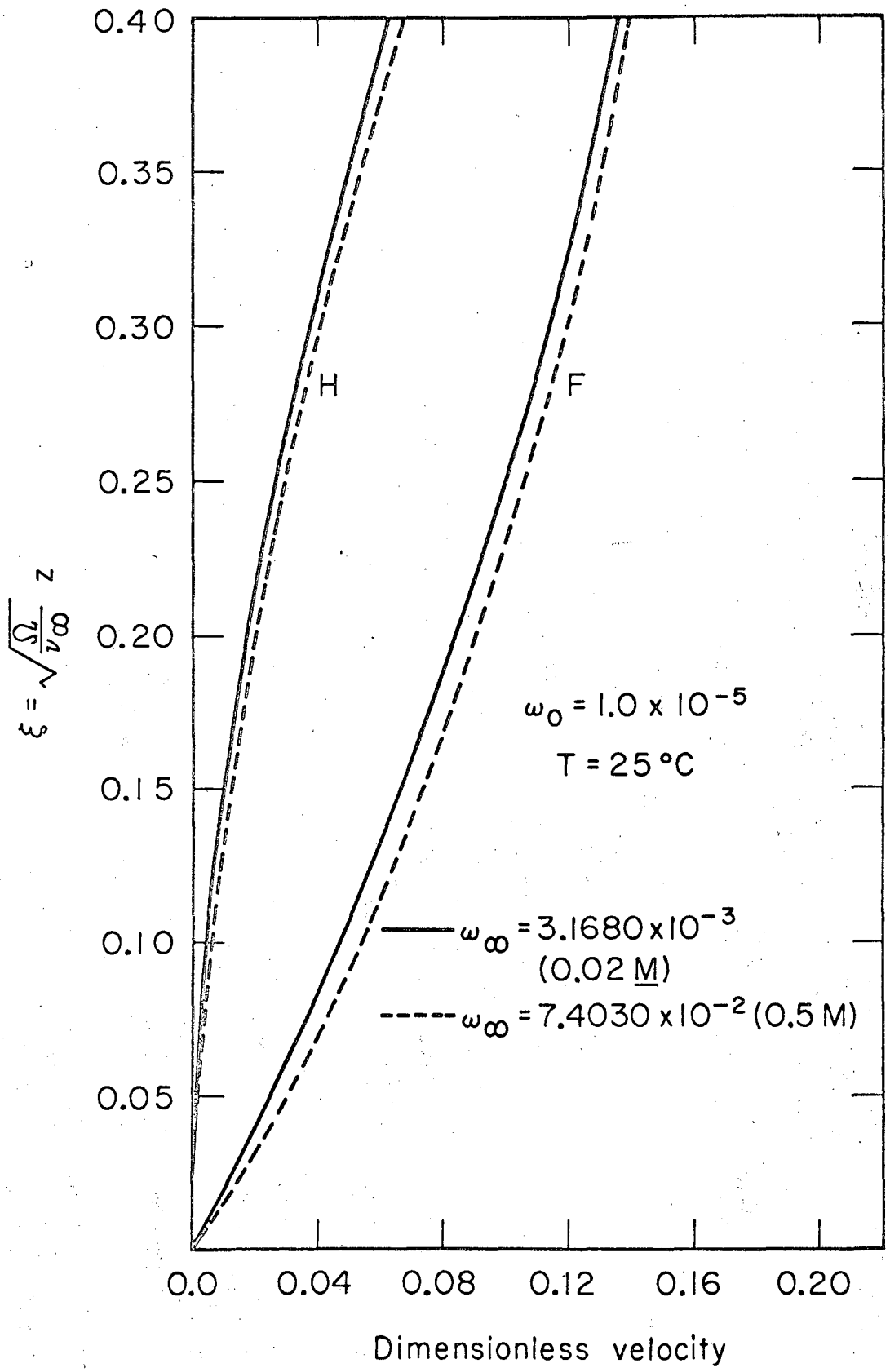

Figure 2-6. Velocity profile in copper sulfate solutions at 25°C.

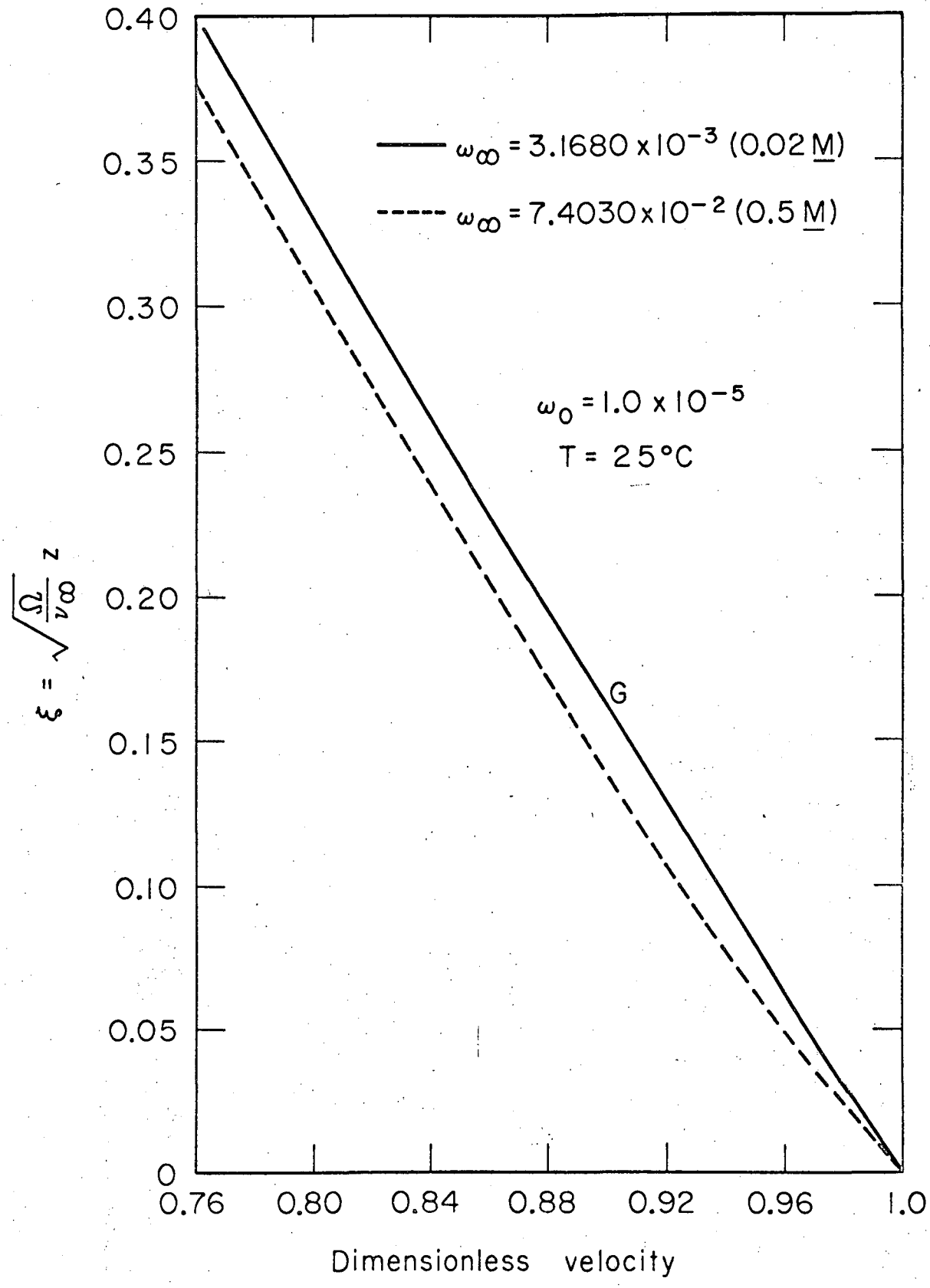

Figure 2-7. Velocity profile in copper sulfate solutions at 25°C.

field in his monograph. Several review papers on the basic ideas of electrode kinetics are due to Parsons[15] and Petrocelli[16].

A fairly general equation which has been used frequently to relate the current density and overpotential for a first order electrode reaction is

$$i = i_1 \left[\frac{C_{ox}}{(C_{ox})_\infty} \exp\left(\frac{\alpha\, nF}{RT}\,\phi\right) - \frac{C_{Red}}{(C_{Red})_\infty} \exp\left(-\frac{(1-\alpha)nF}{RT}\,\phi\right)\right] \qquad (3\text{-}1)$$

where i_o exchange current density

α transfer coefficient

C_{ox} concentration of oxidized species at the interface

$(C_{ox})_\infty$ concentration of oxidized species at the bulk solution.

The model and theory for this equation are by no means rigorous. However, it has been widely accepted for fitting experimental results. The main reason it fits the curve so well is that two parameters α and i_o may be adjusted to match the data. They are so flexible that for the same electrode system the values of i_o frequently differ from author to author. Tanaka and Tamamushi[17] have collected most available kinetic parameter data and tabulated them. They also complained that it was hard to compare the data on the same system obtained by different investigators by different methods.

The total overpotential is usually regarded as the sum of activation overpotential ϕ_a, the concentration overpotential ϕ_c, and the ohmic resistance of the solution ϕ_{ohm},

$$\phi_{tot} = \phi_a + \phi_c + \phi_{ohm} \,. \qquad (3\text{-}2)$$

In Equation (3-1), ϕ presumably is the sum of ϕ_a and ϕ_c. There is essentially no clear-cut line between ϕ_a and ϕ_c. It depends on how they were defined.

Petrocelli[16] separated the concentration overpotential from ϕ_a by assuming that $\phi = \phi_c$ when the applied current i is much less than i_o. Physically, this means that the electrode reaction is proceeding very close to equilibrium and the overpotential is due almost entirely to the concentration change and was designated by ϕ_c. Whereas, ϕ_a was claimed by him to be the remaining part, i.e.,

$$\phi_a = \phi - \phi_c .$$

We will not follow his method. It is mentioned here simply for the purpose of comparison. The distinction we draw between ϕ_a and ϕ_c is clarified in sections 3-1 and 3-2.

In the absence of concentration polarization, the electrical resistivity of the solution may be taken as constant throughout the solution. The rigorous way to find the total resistance of solution lies in the theory of the potential and involves solving Laplace's equation $\nabla^2\phi = 0$ for the potential with consideration of the geometry of the electrode and insulator as boundary conditions. Kasper[18] gives an excellent review of this field.

An additional contribution to the ohmic resistance arises when there is concentration polarization because the concentration variations in the diffusion layer change the conductivity of the solution. See Figure 3-1 for a schematic representation of the electrical resistivity in the solution. This additional resistance has been considered as a part of the concentration polarization in this paper.

§3-1 Concentration Overpotential

It has long been realized that when two identical single electrodes are in contact with different concentrations of solution, there exists

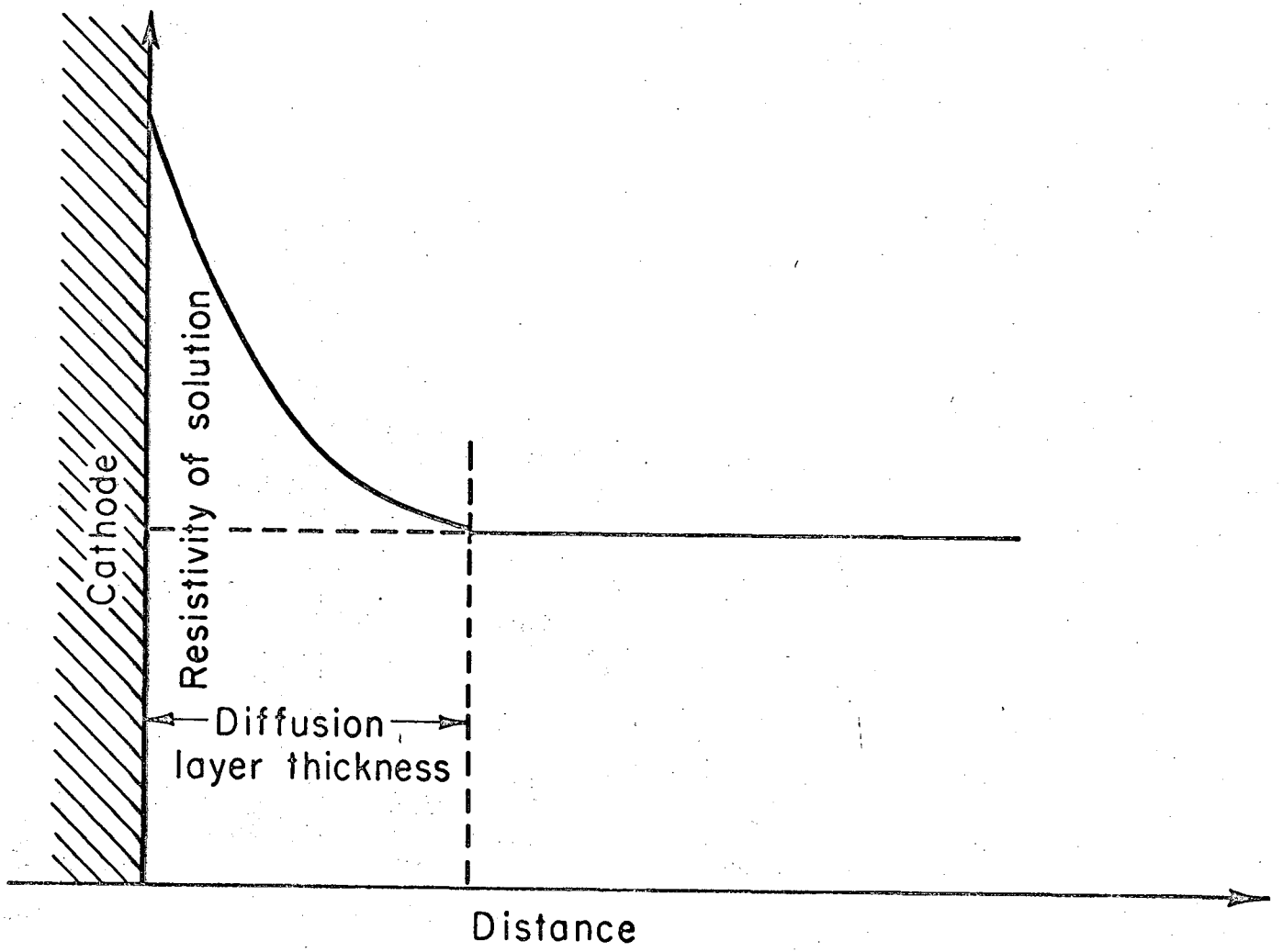

Figure 3-1. Resistivity in solution near the electrode surface. Dash line: shows the resistivity in the absence of concentration changes.

an e.m.f. between the two terminals. When an electrochemical process takes place at the surface of an electrode, the slowness of supply of ions by diffusion and migration produces a concentration gradient, or chemical potential gradient in the thermodynamic sense between the bulk solution and the interface near the surface of the electrode. This means that the applied potential must be large enough to balance the e.m.f. produced by the concentration difference in addition to the other voltage drops in the circuit.

Also there is another effect which arises due to the concentration gradient in the diffusion layer. It is the change of electrical conductivity in the diffusion layer as was mentioned in the beginning of this chapter.

A general equation of concentration overpotential which includes both effects was presented by Newman[12]. In general an electrode reaction in a binary salt solution can involve the solvent and the ions

$$S_+Q_+^{z_+} + S_-Q_-^{z_-} + S_oQ_o \rightarrow ne^- \qquad (3\text{-}3)$$

where Q_i symbol for the formula of species i

S_i the stoichiometric coefficient of species i.

In this case the potential gradient in the solution for such a reference electrode referred to a reference electrode at a fixed location is[12]

$$\nabla\phi = -\frac{1}{\kappa} - \frac{1}{Fz_+\nu_+}\left(\frac{z_+S_+}{n} + t_+ - \frac{S_oz_+C_+}{n\,C_o}\right)\nabla\mu_e \qquad (3\text{-}4)$$

where $\nabla\mu_e$ is the chemical potential gradient which equals $(\nu_+ + \nu_-)RT\nabla \ln \gamma m$, γ is the activity coefficient of the salt, m is the molality of the solution, and κ is specific conductivity of the solution.

As it has been assumed in section 2-1 that the physical properties of the solution in the diffusion layer are functions of z only, so are the electrical potential ϕ and chemical potential μ_e:

$$\nabla\phi = \frac{d\phi}{dz} = -\frac{1}{\kappa} - \frac{(\nu_+ + \nu_-)RT}{Fz_+\nu_+}\left(\frac{z_+S_+}{n} + t_+ - \frac{S_o z_+ C_+}{n\,C_o}\right)\frac{d\,ln\,\gamma m}{dz}\,. \qquad (3\text{-}5)$$

Introduction of the dimensionless distance ξ and dimensionless current density I, and integration with respect to ξ yields

$$\phi(\xi) - \phi(0) = -\frac{\nu_\infty I\rho_\infty \nu_+ Fz_+}{M_s}\int_0^\xi \frac{1}{\kappa}\,d\xi - \frac{(\nu_+ + \mu_-)RT}{Fz_+\nu_+}\int_{(\gamma m)_o}^{(\gamma m)_\xi}\left(\frac{z_+S_+}{n} + t_+ - \frac{S_o z_+ C_+}{n\,C_o}\right)\frac{d\gamma m}{\gamma m}. \qquad (3\text{-}6)$$

The concentration overpotential is then defined as the difference between this total potential difference and the ohmic drop in a nuniform solution of conductivity κ_∞:

$$\phi_c = \frac{\nu_\infty I\rho_\infty \nu_+ Fz_+}{M_s}\int_0^\infty \left(\frac{1}{\kappa} - \frac{1}{\kappa_\infty}\right)d\xi + \frac{(\nu_+ + \nu_-)RT}{Fz_+\nu_+}\int_{(\gamma m)_o}^{(\gamma m)_\infty}\left(\frac{z_+S_+}{n} + t_+ - \frac{S_o z_+ C_+}{n\,C_o}\right)\frac{d\gamma m}{\gamma m}. \qquad (3\text{-}7)$$

§3-2 Activation Overpotential

According to the Arrhenius theory of chemical kinetics, a chemical reaction occurs when a sufficient driving force is provided to cause the reactants to overcome a certain energy barrier and reach an activated state, thus initiating the reaction. Similarly, for an electrode reaction, a potential must be applied in order to change the shape of the energy barrier such that it favors the electrode reaction in one direction rather than the other. This part of the overpotential which is used to overcome the activation energy barrier is called the activation overpotential. It is also said to be related to the slowness of the chemical step or the charge transfer at the electrode.

Jahn and Vielstich[19] have used the rotating disk electrode to study the rates of electrode reactions. They claim that the activation overpotential can be measured by extrapolating the rotating speed to infinity. Physically, this means that the electrolyte is so well stirred that there is no concentration difference being set up at the interface when a current is passing through it. There would be no concentration overpotential if there is no concentration difference. This is to say that if $C_i = (C_i)_\infty$, the overpotential is all due to activation overpotential, and Equation (3-1) becomes

$$i = i_o \left[\exp\left(\frac{\alpha\, nF}{RT}\, \phi_a\right) - \exp\left(-\frac{(1-\alpha)nF}{RT}\, \phi_a\right)\right] \qquad (3\text{-}8)$$

where ϕ_a is activation overpotential.

§3-3 Resistance Overpotential

For a disk electrode submerged into an electrolytic solution, the ohmic drop has been ignored by most workers[8,19,20,21]. They all add a large amount of supporting electrolyte in order to increase the conductivity of solution and minimize the ohmic drop.

However, for a disk electrode, 5 mm in diamter, in a solution of specific conductivity as high as 0.1 $ohm^{-1}cm^{-1}$, the ohmic drop has almost the same order of magnitude as concentration and activation overpotential for many electrode reactions.

Levich[2a] made an attempt to find the ohmic resistance by assuming that the potential is a function of normal distance from the disk only. Presumably, the disk has an infinite diameter. However, it turns out to be a very poor assumption for a disk of finite size.

Applying the theory of the potential, Newman[22] solved Laplace's equation for the electric potential by using oblate spheroidal coördinates.

Surprisingly, for a small disk embedded in the surface of an insulator and a counter electrode which is located far from the disk, the ohmic resistance of a uniform solution is simply equal $\frac{1}{4r_o\kappa}$ where r_o is the radius of the disk electrode.

Furthermore, the resistance in the solution corrected to account for the placement of a reference electrode at a finite distance from the disk is given by

$$R = \frac{\tan^{-1}\lambda_o}{2\pi\, r_o\, \kappa} \tag{3-9}$$

where λ_o is dimensionless distance in spheroidal coördinates between the reference electrode and the rotating disk electrode. It is defined, in terms of cylindrical coördinates, as

$$\lambda_o = \frac{z}{r} \qquad \text{at } r = 0 \text{ (on the axis of the disk)} \tag{3-10}$$

$$\lambda_o = \sqrt{\left(\frac{r}{r_o}\right)^2 - 1} \qquad \text{at } z = 0, r \geq r_o \text{ (in the plane of the disk)} \tag{3-11}$$

For any other arbitrary points, λ_o can be solved from

$$r_o^2\,\lambda_o^4 + (r_o^2 - r^2 - z^2)\,\lambda_o^2 - z^2 = 0\,. \tag{3-12}$$

Figure 3-2 shows the equipotential lines and current flow lines near to a disk electrode. In Figure 3-3 the dimensionless group $r_o\kappa R$ is plotted against λ_o, and it is seen that the resistance depends strongly on distance in the region near the disk electrode. The proper choice of the position of a reference electrode based on these results will be discussed in section 4-2.

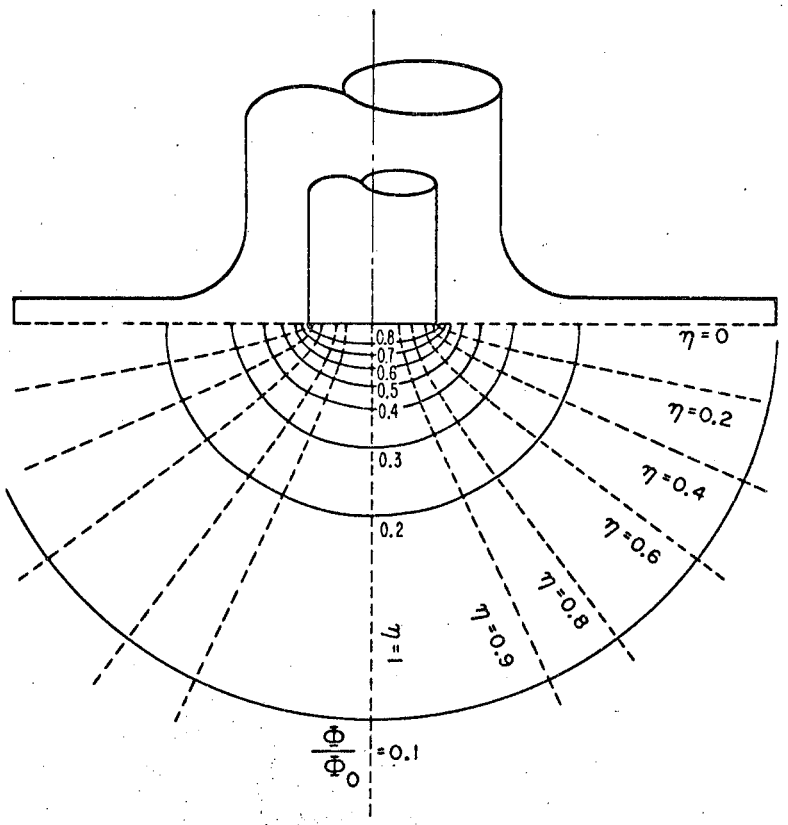

Figure 3-2. Equipotential lines and current flow line near a disk electrode.

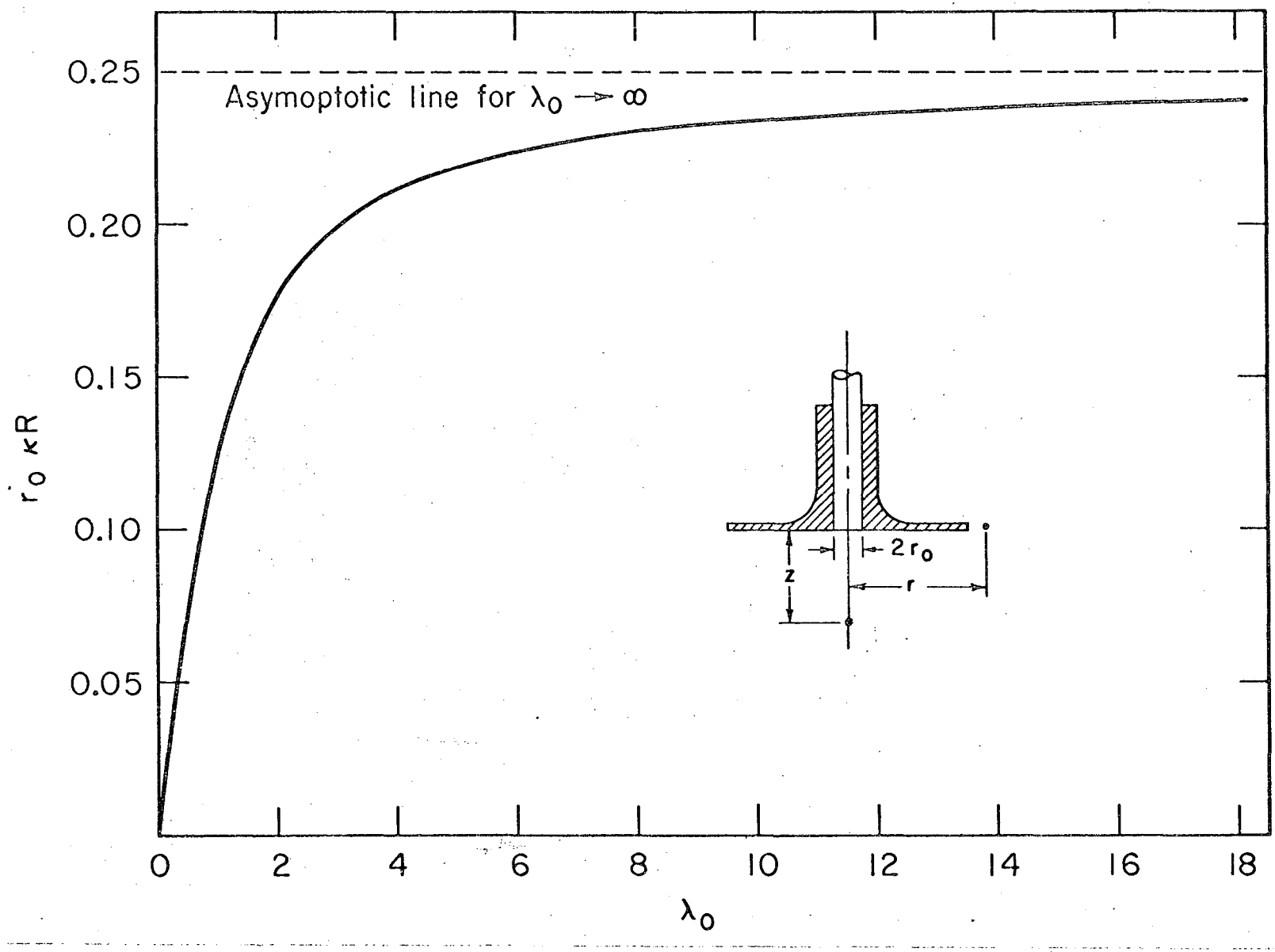

Figure 3-3. Correction to the resistance of the solution for the finite distance of the reference electrode.

$\lambda_o = z/r$ on the axis of disk

$\lambda = \sqrt{\left(\frac{r}{r_o}\right)^2 - 1}$ in the plane of disk

VI. EXPERIMENTAL WORK

§4-1 Design and Description of Apparatus

Cathode (Rotating Disk Electrode)

The size and the shape of the rotating disk electrode is important, since it may affect the flow pattern. Riddiford[3] summarized various shapes of disk which have been used in the past by different experimenters. In general, if there is no effect which may propagate backward from the edge of the disk and change the fundamental hydrodynamic model and concentration profile near the surface of disk, it may be considered to satisfy the original assumptions in the basic theory.

The shape recommended by Riddiford and also the one being used in this work is shown in Figure 4-1. Only the central portion of the upper surface is active.

Several criteria have been set up by Riddiford and by Theodorsen and Regier[23] for the actual design of the size of the electrode. They are:

1. the outside diameter of disk d should be greater than the hydrodynamic boundary thickness;

2. the diameter of the working surface d_o should be greater than the mass transfer boundary layer thickness;

3. the size of the shaft should be less than 30% of the size of the disk, so that the shaft will not affect the main stream of flow;

4. the thickness of the disk should be less than 1/30 of the disk size, so that there will be no edge effect;

5. the Reynolds number at the edge should be less than 2×10^5 in order to maintain laminar flow.

The disk has been carefully designed to meet the requirements

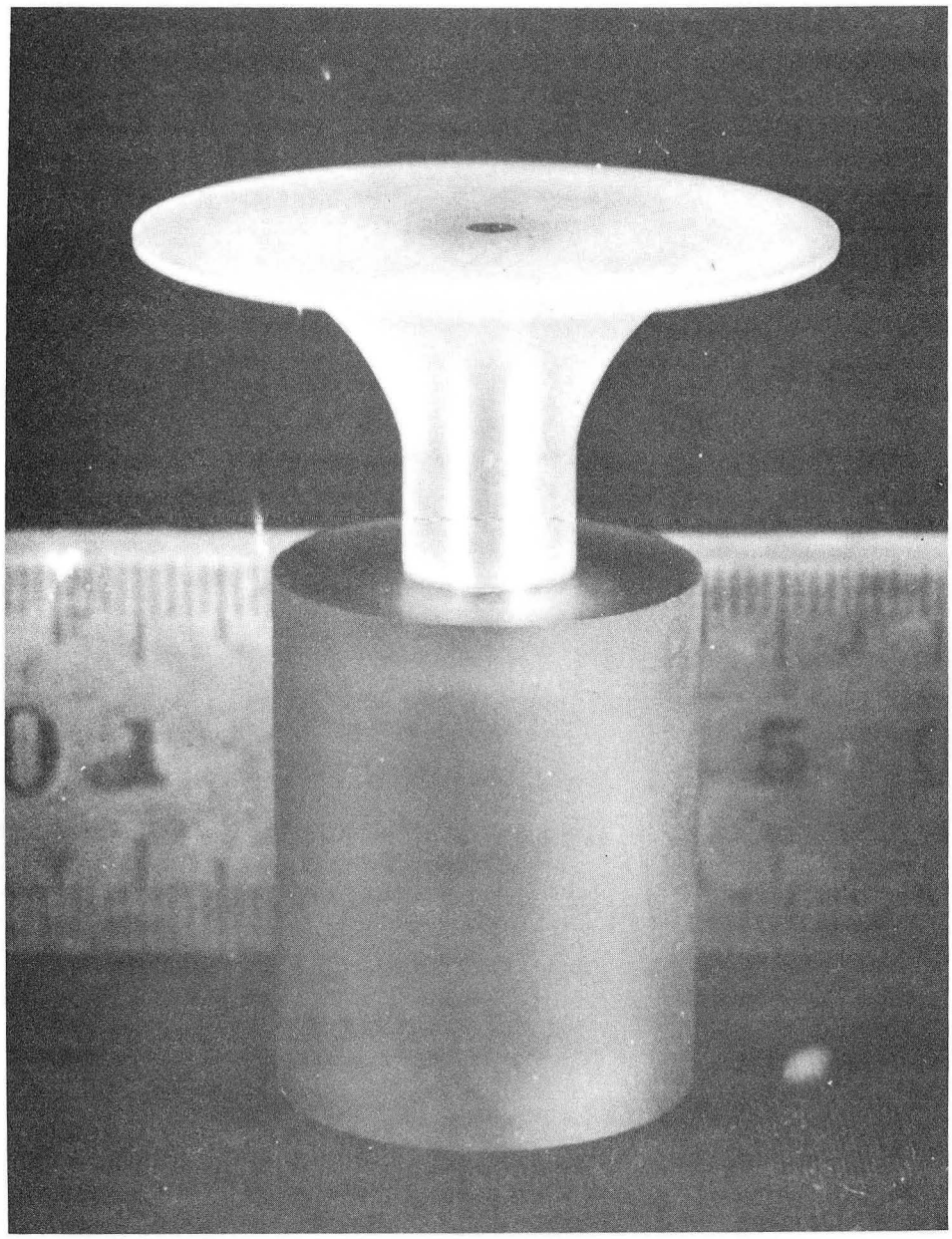

ZN-5395

Figure 4-1. Disk electrode.

listed above. The disk is operated in $CuSO_4$ solution with the speed range from 60 r.p.m. to 500 r.p.m. Here are the specifications of the disk:

Outside diameter of disk,	$d = 4$ cm
Working electrode diameter,	$d_o = 0.5$ cm
Disk thickness,	$= 0.1$ cm
Shaft diameter	$= 1$ cm.

The central part of the electrode was machined from oxygen-free high purity copper to precise dimensions and then embedded in an epoxy resin cast. It was further machined to the desired shape.

The disk was attached to a spindle which was tightly fitted in two 7/8-inch o.d. New Departure 77 RC bearings. These bearings were mounted to a heavy brass bearing case in order to keep the eccentricity as small as possible. The eccentricity at the edge of disk was measured to be less than 0.002 inch.

Anode

The anode was designed to provide an area more than 100 times bigger than the cathode for the purpose of minimizing the anodic overpotential. The anode was embedded at the bottom of the vessel and could be taken apart to clean the surface before each experiment. It was made liquid tight with a rubber ring placed in a groove.

Reference Electrode

An oxygen-free high purity copper rod was used as the reference electrode. It was connected to the electrolyte cell through a capillary tube filled with electrolytic solution with the same concentration as in the cell. The capillary had a fine tip which faced downward and was located at the side of rotating disk. The use of a copper ference electrode was desirable since it would not contaminate this electrolyte and involved

no liquid junctions.

§4-2 The Position of Reference Electrode

As it was mentioned at the beginning, there was no supporting electrolyte in this work, and the electrical conductivity was very low compared to most other works in this field. A high ohmic drop may seriously interfere with the overpotential measurement. To minimize the resistance in overpotential measurements, Brown and Thirsk[8], Johnson and Turner[20], and Ibl and Schadegg[24] placed their reference electrode directly underneath the disk. This arrangement may seriously disturb the hydrodynamic profile and current distribution under the rotating disk electrode. Belyaeva[25] made some improvements on the design of a rotating disk by building the reference electrode inside the disk with a small hole (dia. 0.5 - 0.7 mm) at the center of the disk electrode which was 4 mm in diameter. This is still not a satisfactory way because of the small hole that still distorts the concentration profile and there is the uncertainty of the concentration inside the rotating disk.

Several preliminary experiments were conducted to measure the overpotential at a constant current density 40.7 mA/cm^2 in a 0.1M copper sulfate solution at 25°C with a rotating speed of 300 r.p.m. with the reference electrode at various distances from the disk. The results are tabulated in Table 1.

These data show that the cathodic overpotential depends strongly on the normal distance of the reference electrode from the disk electrode. For these cases where the reference electrode was placed underneath the disk or built into the rotating disk, a small misalignment in the position of the reference electrode from one experimental run to the next may cause

a serious difference in the ohmic drop contribution to the total overpotential measurement.

Table 1 also shows that the resistance overpotential is almost as large as the total cathodic overpotential. The difference between the experimental value of total overpotential and the calculated value of resistance overpotential is about 70-80 mV and is the sum of activation and concentration overpotential under these experimental conditions.

From both the theoretical analysis in section 3-3 and the experimental results in Table 1, we concluded that the reference electrode should be placed sufficiently far from the disk, e.g., $\lambda_o > 10$. The distance parameter λ_o was defined in Equation (3-10) to (3-12).

§4-3 Surface Treatment of Electrode

Because of the inevitability of surface change during a metal deposition reaction, we need to know how smooth the electrode surface should be or what is the maximum tolerable roughness in order to maintain the theoretically expected velocity profile.

Schlichting[26] gave a systematic presentation and study of the effect of surface roughness. Generally speaking, a surface may be considered hydraulically smooth if the roughness is smaller than the hydrodynamic boundary layer for the case where there is no mass transfer occurring at the surface.

Brown and Thirsk[8], and Beacom and Hollyer[27] worked on rotating disk electrodes with the same electrolytic system as the author. The former used electron micrographs and found a deposited copper film with a surface roughness negligible when compared with the diffusion layer. On the other hand, Beacom and Hollyer measured the copper deposition by interference microscope and found a uniform deposit on the disk.

Table 1. The cathodic overpotential with respect to normal distance from the disk electrode

$c = 0.1$ M $CuSO_4$ $\quad A = 0.1962\ cm^2$

$\Omega = 300$ r.p.m. $\quad r_o = 0.25$ cm

$i = 40.7\ mA/cm^2$ $\quad \kappa = 0.00872\ cm^{-1}ohm^{-1}$

Normal distance	Resistance Overpot. calculated from Fig. 3-3	Experimental result
0.1 cm	224 mV	290-300 mV
0.2 cm	392 mV	461-465 mV
0.3 cm	546 mV	620 mV
0.5 cm	646 mV	721 mV
2.0 cm	845 mV	924 mV
5.0 cm	892 mV	965 mV
beside the disk (r = 2.5 cm)	866 mV	942 mV

Ibl and Schadegg[24] characterized the roughness of copper deposition by impedance measurements. They found that there is essentially no formation of a roughness or powdery deposit if the copper is deposited below the limiting current. On the other hand, a very rough deposit was formed at limiting current or higher even with a strong stirring of the solution.

An extensive study on the effect of small protrusions on mass transfer to a rotating disk electrode was given by Rogers and Taylor[28]. Their autoradiographic results, with carbon-14 as a tracer showed that the mass transfer rate is lower in the traces of wakes behind burrs or gas bubbles. However, it is compensated by the slight increase of available area of the small protrusions. Hence there is no significant difference in the total rate of mass transfer between the one with burrs and the one without burrs.

Karasyk and Linford[29] studied the effect of organic contaminants on the electrode surface to the polarization curve of copper plated from an acid copper sulfate bath. They found that trace contaminants cause a reduction in the double layer capacity, and consequently the polarization curves are much steeper than those for clean ones.

We concluded that in order to maintain hydrodynamic smoothness of the electrode surface, the polariztion measurement should be conducted below the limiting current density. Once a surface reaches the limiting current density, it should be retreated before being used for further measurement.

The maximum roughness should be less than the diffusion layer thickness. From the theoretical analysis of the concentration profile, the diffusion layer thickness for a disk electrode at 300 r.p.m. in a

0.1M copper sulfate solution is 37.1×10^{-3} cm.

Summarized below are the steps in treating the surfaces of the cathode, the anode, and the reference electrode before conducting each experiment:

1. The electrodes were polished with 600-A silicon carbide paper until all previous traces of deposit or corrosion were gone. The maximum scratch on the surface is then on the order of 10 μ (10^{-3} cm).

2. The cathode was further polished on plate glass using fine lens powder (aluminum oxide powder mixture) of 0.3 μ grain size as grinding compound.

3. The electrode was washed with carbon tetrachloride followed by 5% sodium carbonate solution.

4. The surfaces were rinsed with tap water followed by distilled water.

§4-4 The Electrical Circuit

The schematic diagram of the circuit for measuring cathodic polarization is shown in Figure 4-2. The current source was a Lambda model 28 regulated power supply. The current flow in the cell was measured with a Keithley Model 610R Electrometer which has an accuracy of 2%. The potential was measured with a Houston Model HV-160 DC vacuum tube voltmeter which has an accuracy of 0.3%. The results were recorded on a t-y recorder.

The electrical connection to the rotating disk electrode was accomplished by means of a mercury well. The disk was rotated with a variable speed motor*, controlled by a precision DC voltage power

---

* Bodine Electric Company, Type NSE 11R, Two shafts AC-DC motor with a gear ration 10 to 1.

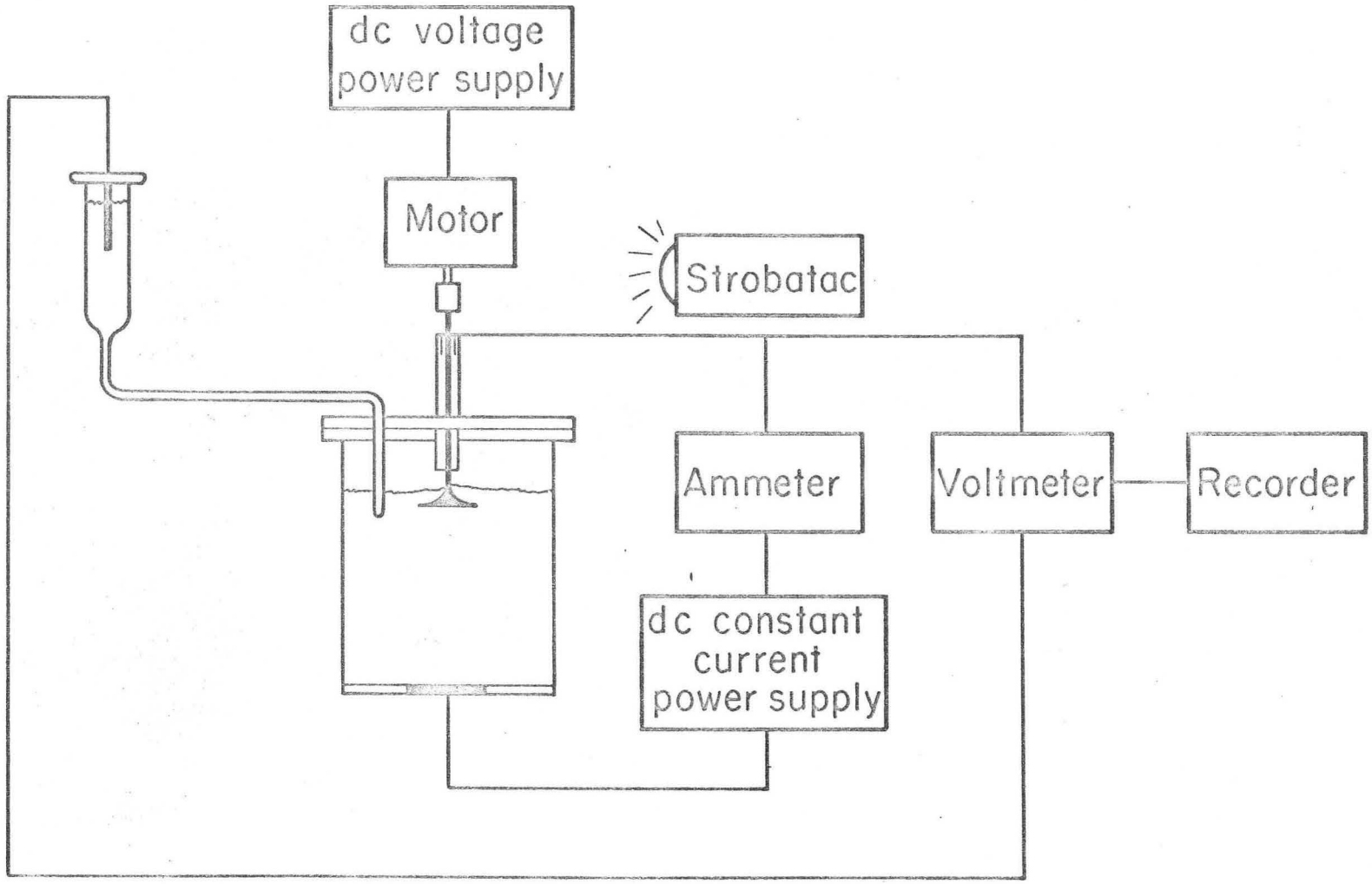

Figure 4-2. The block diagram of the rotating disk electrode system.

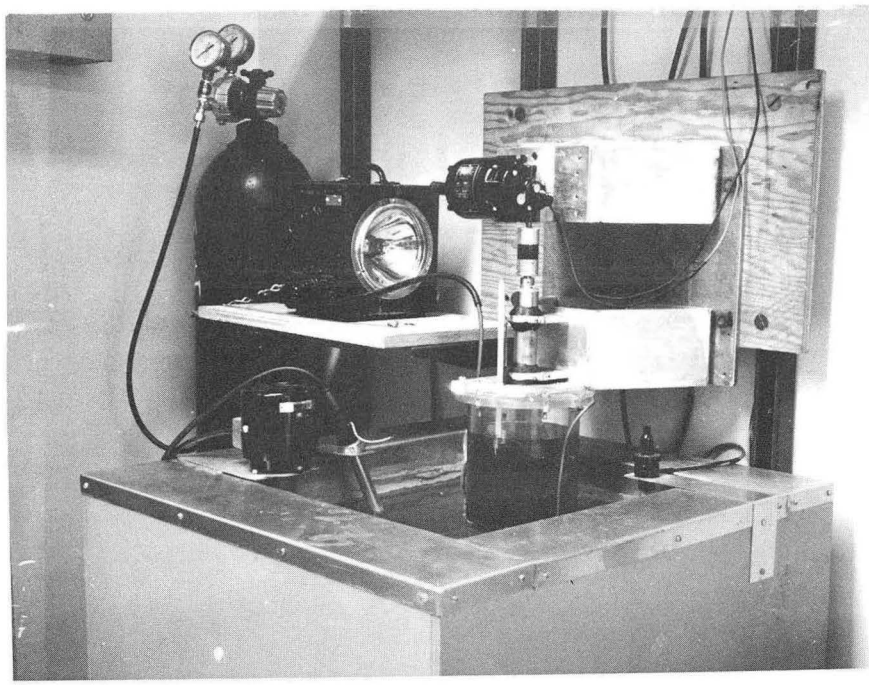

Figure 4-3. The rotating disk electrode set up.

supply*. The speed of rotation was determined by a General Radio Type 631-BL strobotac which has an accuracy of 1%.

Figure 4-3 shows the assembled rotating disk electrode apparatus.

§4-5 Experimental Procedure

Reagent grade $CuSO_4$ was used without further purification. Distilled water was used in the preparation of all solutions. Cylinder nitrogen was bubbled through the solution to expel all dissolved oxygen which may affect the surface of the electrode during the reaction.

Before each run, the surfaces of the electrodes were cleaned as described in section 4-3.

Because of the high ohmic drop in the solution compared with the concentration and activation overpotential, the plateau on the current voltage curve due to concentration polarization was essentially overshadowed, and it was difficult to locate the limiting current density by a current vs. voltage measurement. Therefore, instead of keeping the rotating speed constant and varying the current density, as most other experimenters have done, we held the current density constant and varied the rotation speed. Thus the resistance overpotential was kept constant throughout a run.

The disk electrode was initially set at a relatively high speed (5-10 times higher than the "limiting speed"). The speed was decreased by decreasing the voltage to the motor which drove the shaft of the disk. The total overpotential was not very sensitive to this decrease of speed at a given current density until it came close to the limiting speed where the potential sharply increased. At this point the rotation speed was measured by a strobotac.

The measurement of limiting speed has the same physical significance

* Power Design Inc., Model 5015A.

as a limiting current density measurement. The limiting current density gives the minimum current required to discharge all the reactive ions brought to the electrode surface at a given speed of rotation, whereas the limiting speed gives the minimum speed required to supply the reacting ions at a given current density. Both measurements correspond to a zero concentration of ions at the electrode surface.

V. RESULTS

1. The limiting speeds ranging from 60 r.p.m. to 500 r.p.m. were measured at constant current density according to the procedure given in the section 4-5. The square root of limiting speed was plotted against current density. Straight lines passing through the origin were obtained for all four concentrations, 0.02M, 0.05M, 0.1M and 0.3M. The slopes of these lines $\frac{i_{lim}}{\sqrt{\Omega}}$, have been compared with the values predicted from Equation (2-28).

This theory gives +1.57% correction to the Levich theory for a copper sulfate solution concentration of 0.02 M, and +13.1% correction at concentration of 0.3 M. The experimental results show a negative deviation at low concentration, but agree well with the value predicted from this theory at high concentration. It reveals the importance of the effects of the variation of physical properties in the diffusion layer and non-zero interfacial velocity at the electrode surface when the rotating disk electrode method is used to measure the diffusion coefficient in a highly concentrated solution.

We may also want to compare our results with the $\frac{i_{lim}}{\sqrt{\Omega}}$ values calculated from Levich's equation where constant physical properties, zero interfacial velocity, and infinite Schmidt number were assumed.

$$\frac{i_{lim}}{\sqrt{\Omega}} = 0.620\ Sc^{-2/3}\ \frac{nF\ C_{\infty}\sqrt{\nu}}{(1 - t_{+})} \qquad (5\text{-}1)$$

and from the modified equation which was given by Gregory and Riddiford[30]

$$\frac{i_{lim}}{\sqrt{\Omega}} = \frac{0.554\ Sc^{-2/3}}{0.8934 + 0.316\ Sc^{-0.36}} \frac{nF\ C_\infty \sqrt{\nu}}{(1 - t_+)} \ . \tag{5-2}$$

Further correction for finite Schmidt number (range from 100 to infinity) was made by Newman[31]. He used the expansion of the velocity profile obtained by Cochran[13] and integrated analytically to obtain

$$\frac{i_{lim}}{\sqrt{\Omega}} = \frac{0.62048\ Sc^{-2/3}}{1 + 0.2980\ Sc^{-1/3} + 0.14514\ Sc^{-2/3}} \frac{nF\ C_\infty \sqrt{\nu}}{(1 - t_+)} \ . \tag{5-3}$$

The numerical comparison of Equations (2-28), (5-1), (5-2), (5-3) and experimental results for copper solutions at 25°C are given in Table 2. They are also shown in Figure 5-1.

2. For the cathodic reaction of copper sulfate at a copper electrode, the electrode reaction is

$$Cu^{++} + 2e \rightarrow Cu \ .$$

Therefore $S_+ = -1$, $S_o = 0$, $n = 2$, $z_+ = 2$ and $\nu = 2$ in Equation (3-3). The potential far away from the electrode was chosen as the reference point; $\phi(\infty) = 0$. Equation (3-7) multiplied by $\frac{F}{RT}$ on both sides of the equation, so that each term is dimensionless, becomes

$$\frac{F\phi_c(0)}{RT} = \frac{\nu_\infty I \rho_\infty \nu_+ F^2 z_+}{RT\ M_s} \int_0^\infty \left(\frac{1}{\kappa} - \frac{1}{\kappa_\infty}\right) d\xi + \frac{(\nu_+ + \nu_-)}{z_+ \mu_+} \int_{(\gamma m)_o}^{(\gamma m)_\infty} (t_+ - 1)\ d\ ln\ \gamma m. \tag{5-4}$$

The first term on the right-hand side represents the additional ohmic resistance due to the conductivity change in the diffusion layer. The integration was performed numerically with the computer. The conductivity at each mesh point was evaluated according to the concentration profile from Equation (2-23).

The second term on the right of Equation (5-4) represents the part

Table 2. Comparison of $\frac{i_{lim}}{\sqrt{\Omega}} \left[\frac{mA}{cm}/\sqrt{\frac{rad}{sec}}\right]$ predicted by different authors with experimental results

c	Sc*	Levich Eq(5-1)	Gregory & Riddiford Eq(5-2)	Newman Eq(5-3)	This theory Eq(2-28)	Exptl. Result
0.02 M	1407	2.995	2.919	2.914	3.042	2.86
0.05 M	1530	6.986	6.814	6.803	7.173	7.04
0.1 M	1650	13.05	12.74	12.72	14.13	14.06
0.3 M	2012	33.71	32.96	32.91	38.12	38.1

* Schmidt number was calculated based on bulk properties of the solution.

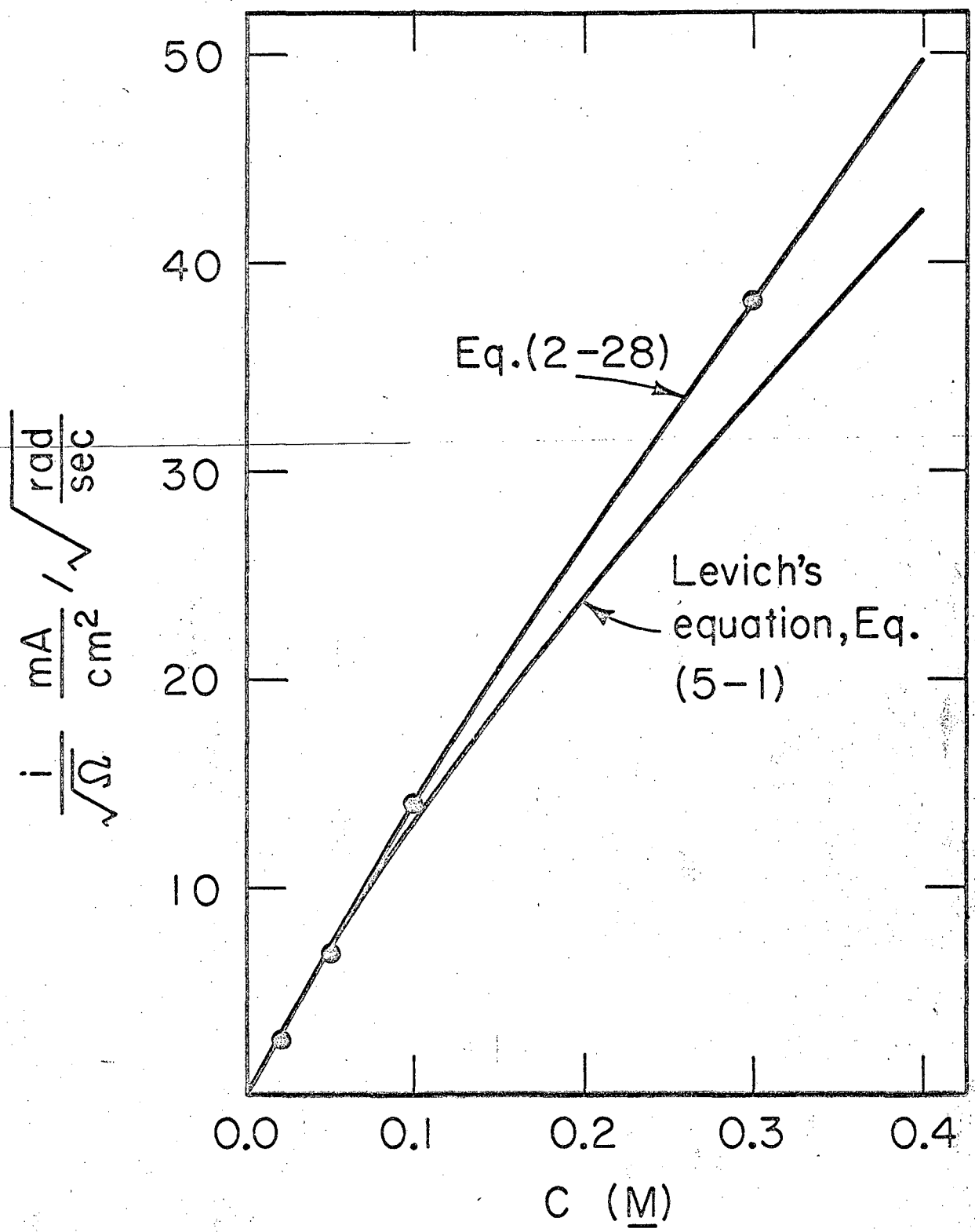

Figure 5-1. Comparison of the exact value of $\frac{1}{\sqrt{\Omega}}$ with Levich's equation and experimental results for $CuSO_4$ solutions at 25°C.

of the potential necessary for overcoming the e.m.f. due to the concentration difference. The integration was performed by changing the variable of integration to ω_s. The cation transference number t_+ and $\log_{10}\gamma$ have been linearly regressed as a finite polynomial of ω_s in 2-4, while the molality m is related to ω by

$$m = \frac{1000\ \omega_s}{(1-\omega_s)M_s}$$

$$\frac{d\ \ln m}{d\ \omega_s} = \frac{1}{\omega_s} + \frac{1}{1-\omega_s} = \omega_s^{-1} + 1 + \omega_s + \omega_s^{-2} \ . \ . \ . \ .$$

There was no difficulty in performing this integration analytically. The result ϕ_c was plotted as a function of $\frac{1}{z_+FC_\infty\sqrt{\Omega\mu_\infty}}$ and is shown in Figure 5-2.

3. According to the classical mass transfer theory for constant properties, the interfacial concentration is related to the current density by

$$\frac{C_o}{C_\infty} = 1 - \frac{i}{i_{lim}} \ .$$

If the ratio $\frac{C_o}{C_\infty}$ is plotted against $\frac{i}{i_{lim}}$, a straight diagonal line should be obtained for each bulk concentration. This equation was tested at different concentrations taking into consideration the effect of variations of physical properties. Figure 5-3 shows that the higher the bulk concentration, the more the results deviate from the diagonal line.

4. For the purpose of comparison of the total overpotential predicted for the theory with the experimental values, several experiments were conducted separately to measure the total overpotential. Figure 5-4 shows one of the examples. The total overpotential was measured in a 0.1 M copper sulfate solution at a constant rotating speed of 300 r.p.m.

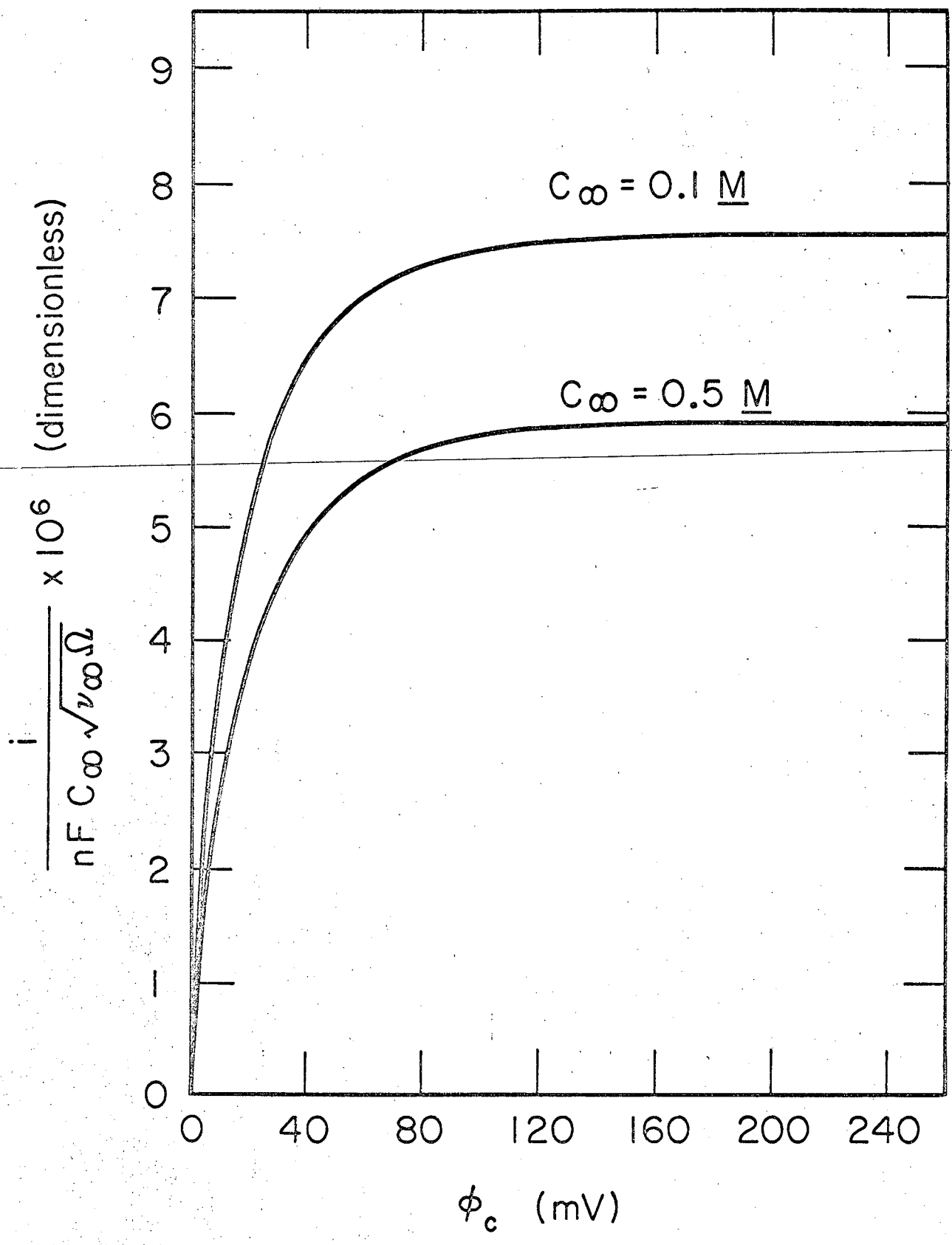

Figure 5-2. Concentration overpotential at different bulk concentration of $CuSO_4$ at 25°C.

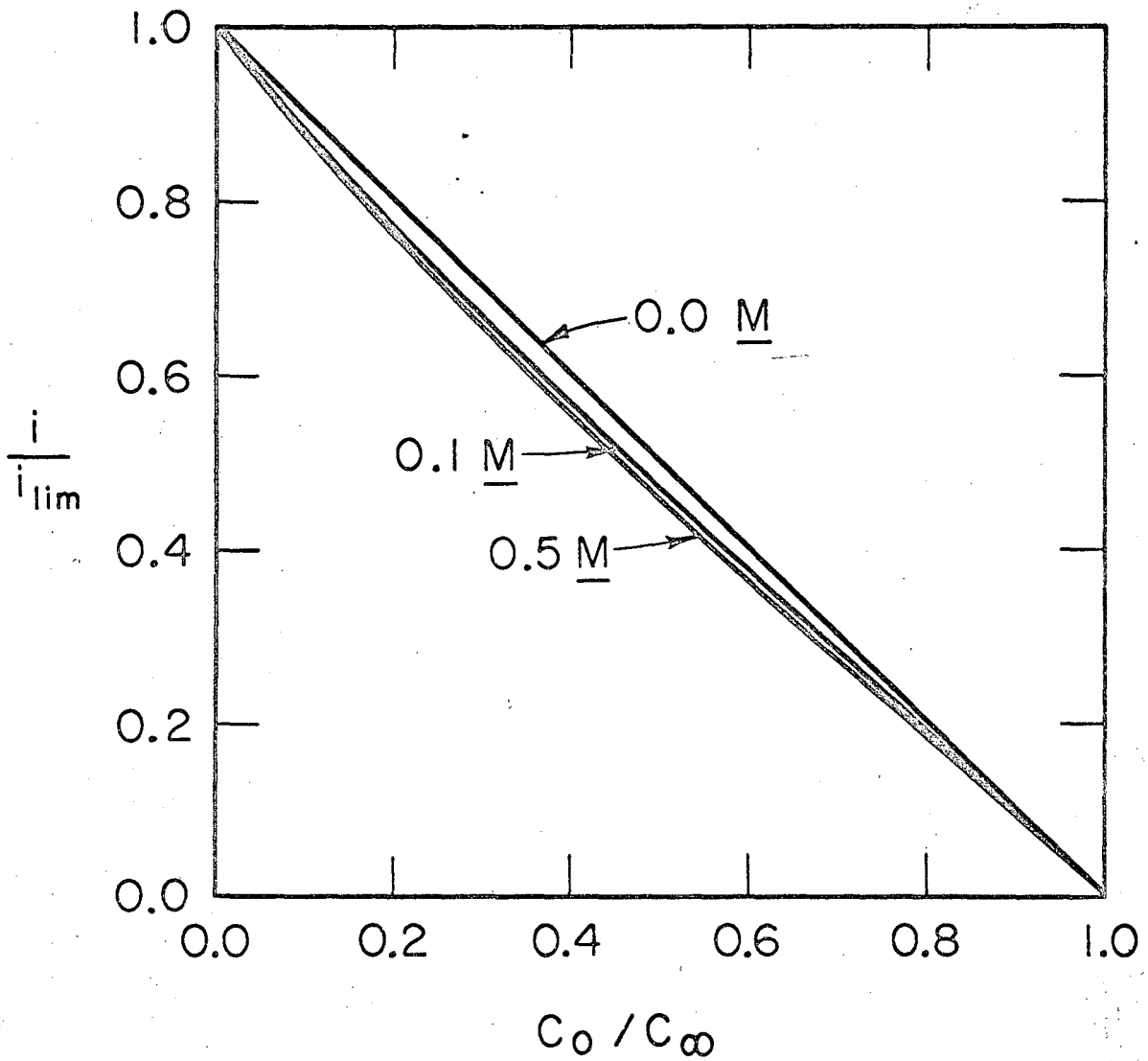

Figure 5-3. Interfacial concentration vs. current density for $CuSO_4$ solutions at 25°C.

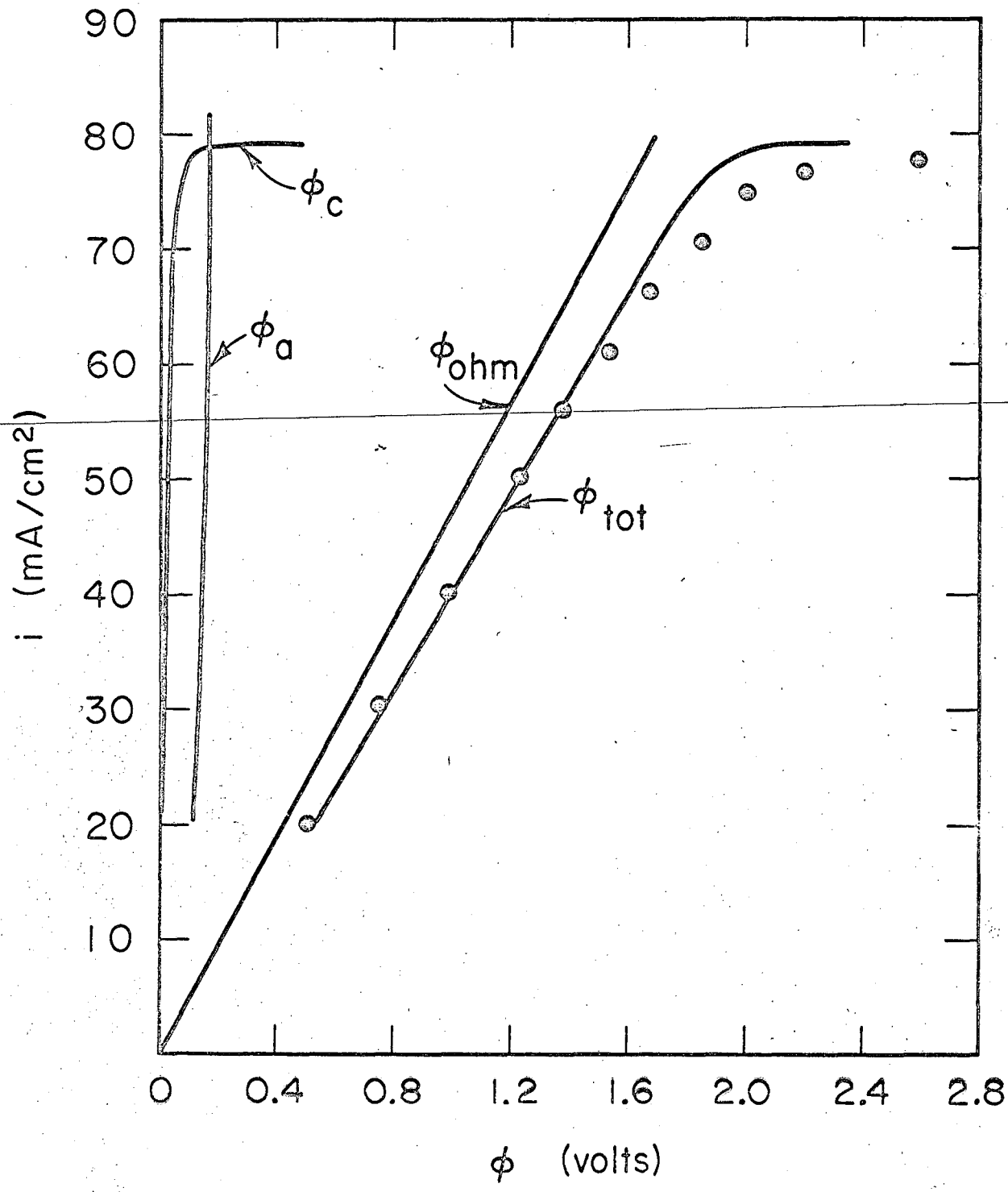

Figure 5-4. Comparison of measured total overpotential to the theoretical value for copper deposition from $CuSO_4$ solutions at 25°C.
Ω = 300 r.p.m. c = 0.1 M

The theoretical concentration overpotential ϕ_c was calculated from the results shown in Figure 5-2. The theoretical activation overpotential ϕ_a was calculated from Equation (3-8); an exchange current density of $i_o = 1.0 \frac{mA}{cm^2}$ and a transfer coefficient of $\alpha = 0.5$[8] were assumed. The resistance overpotential ϕ_{ohm} was calculated from Equation (3-9) taking account of the fact that the reference electrode probe was located in the plane of the disk 2.5 cm from the axis of rotation, that is, $r = 2.5$ cm and $r_o = 0.25$ cm in Equation (3-11) for calculating the parameter λ_o. The specific conductivity of the solution was 0.00872 $ohm^{-1}cm^{-1}$. The theoretical total overpotential is the sum of ϕ_a, ϕ_c , and ϕ_{ohm}.

In view of Figure 5-4, we may see that the resistance overpotential predominates the overall polarization measurement. Therefore, if we wish to study the electrode kinetics in a low conductivity electrolyte, the two large numbers, the measured overpotential, and the resistance overpotential must be subtracted with a consequent loss of significant figures. Therefore, unless a highly accurate voltmeter is available, the rotating disk electrode method is not suitable for kinetic studies in a low conductivity electrolyte.

VI. SUMMARY AND CONCLUSIONS

1. Compared to Levich's early treatment[1] of the rotating disk electrode, two major differences arise in the study of mass transfer in a <u>concentrated</u> electrolyte: the physical properties of the solution vary across the diffusion layer, and the interfacial velocity can no longer be considered to equal zero.

2. In view of these differences, more general forms of the equation of motion, Equation (2-1), and the equation of continuity, Equation (2-3),

than those considered by von Kármán and Levich must be used to calculate the velocity profiles in the vicinity of the rotating disk. In solving these equations, the z-component velocity was assumed to be a function of the normal distance from the disk only. This assumption allowed the set of partial differential equations to be simplified to a set of ordinary differential equations, which were solved numerically by the computer.

3. For the solution of a single salt, the concentration profile is determined from Equation (2-18). The concentration and all the physical properties of solution have also been assumed to be functions of the normal distance only in solving the said equation.

4. It is found that the limiting current is still proportional to the square root of rotating speed even at high concentrations. The experimental results of $\frac{i_{lim}}{\sqrt{\Omega}}$ plotted against the bulk concentration were found to agree well with those predicted from this theory. The theory predicts a value 13% higher than the Levich equation for a 0.3 M copper sulfate solution.

5. Perhaps the most important assumption involved in the rotating disk electrode method is that v_z, c, ϕ and all physical properties of the solution are functions of the normal distance only. There is no doubt for very large disks. Practically, it is impossible to construct such a disk without creating turbulence at the edge of the disk.

If we are interested only in the region very close to the electrode, then this assumption holds quite well. One may visualize this fact from the equal potential lines plotted in Figure 3-2. Near the disk the equal potential lines are parallel to the disk, but the assumption becomes poorer farther from the disk.

A similar picture of equal concentration lines may be obtained if there is no convection, that is, if the concentration satisfies the equation $\nabla^2 C = 0$. If convection diffusion and migration are involved, the equation for a binary electrolyte with the assumption of constant physical properties becomes[1]

$$v \cdot \nabla C = D \nabla^2 C \ .$$

It may be expected that the convection compresses the equal concentration lines in the diffusion layer. The thinner the diffusion layer, the less the error involved in the assumption that the concentration is a function of normal distance. A similar conclusion should hold for v_z.

6. The concentration overpotential was defined as the overpotential due to the concentration gradient in the diffusion layer. It includes two contributions due to the difference of the chemical potential between the bulk and electrode surface, and the change of the electrical conductivity in the diffusion layer.

7. In the absence of supporting electrolyte, the ohmic resistance contribution to total overpotential is very high. The ohmic drop between a small disk embedded in the surface of an insulator and a counter-electrode far from the disk is $\frac{1}{4\kappa r_o}$ [22]. The ohmic resistance corrected to account for the placement of a reference electrode at a finite distance $\frac{\tan^{-1}\lambda_o}{2\pi\, r_o\, \kappa}$. The distance parameter λ_o was defined in Equations (3-10) to (3-12). Because the ohmic drop is concentrated near the disk, the reference electrode should be placed sufficiently far from the disk that its location is not a highly critical factor.

8. The large ohmic drop essentially overshadowed the plateau on the current-voltage curve due to the concentration polarization. This led to the development of a "limiting speed" technique rather than

limiting current measurements. The current was held constant and the rotating speed was decreased until the potential showed a large increase corresponding to a zero concentration of the reacting ion at the electrode surface. In this way the ohmic potential drop was held constant and did not obscure the concentration polarization effects.

In conclusion, the effects of the variation of physical properties in mass transfer to a rotating disk electrode are important in a concentrated solution. It is not recommended to use the rotating disk electrode for the electrode kinetic study in a low conductivity electrolyte where the ohmic resistance dominates the total overpotential.

ACKNOWLEDGMENTS

I wish to express my deep gratitude to Professor J. Newman for initiating my thinking and for the patient instruction in this work. Gratitude is also due to Professor C. W. Tobias and Mr. Thomas Chapman for their useful advice and to Mr. Larry Horvath for his help in setting up the experimental apparatus.

I wish to express my appreciation to the Lawrence Radiation Laboratory for the use of needed experimental equipment, and to Mrs. Jane Schroeder for typing the final manuscript.

This work was done under the auspices of the United States Army Signal Corps and of the United States Atomic Energy Commission.

APPENDIX A. SOME BASIC RELATIONS FOR BINARY ELECTROLYTES

An electrolytic solution containing only one kind of cation and one kind of anion in addition to the solvent is called a binary electrolyte. Some basic relations which have been used for deriving most of the fundamental equations in this paper may be summarized as follows:

Let the electrode reaction at a reference electrode be

$$S_+Q_+^{z_+} + S_-Q_-^{z_-} + S_oQ_o \rightarrow ne^-$$

and let

C_+, C_-, C_o be concentration of cation, anion, and solvent

ν_+, ν_- be number of cations and anions produced by dissociation of one molecule of electrolyte.

The following relations hold for binary electrolytes. We present them without proof.

$$\nu_+ z_+ + \nu_- z_- = 0 \tag{A-1}$$

$$\frac{C_+}{\nu_+} = \frac{C_-}{\nu_-} = C \tag{A-2}$$

$$S_+ z_+ + S_- z_- = -n \tag{A-3}$$

$$\begin{aligned} C_+ M_+ &= \rho\omega_+ \\ C_- M_- &= \rho\omega_- \end{aligned} \tag{A-4}$$

$$M_s \equiv \nu_+ M_+ + \nu_- M_- \tag{A-5}$$

$$\begin{aligned} \mu_e &\equiv \nu_+ M_+ + \nu_- M_- \\ &= (\nu_+ + \nu_-)\, RT \ln \gamma m \end{aligned} \tag{A-6}$$

$$\begin{aligned} \omega_s &= \omega_+ + \omega_- \\ &= \frac{1}{\rho}\,(C_+ M_+ + C_- M_-)\,. \end{aligned} \tag{A-7}$$

Finally, at constant temperature and pressure, the Gibbs-Duhem relation for a binary electrolyte is

$$C_+\nabla\mu_+ + C_-\nabla\mu_- + C_o\nabla\mu_o = 0 \tag{A-8}$$

or

$$C\nabla\mu_e = - C_o\nabla\mu_o \, .$$

APPENDIX B. COMPUTER PROGRAM

The original computer program written for the numerical solution of velocity and concentration profiles has several slight differences in the definitions of the dimensionless quantities.

The dimensionless distance was defined as (cf. Equation (2-10))

$$\zeta = \sqrt{\frac{\Omega}{\mu_o\rho_o}} \int_o^z \rho dz \tag{B-1}$$

and the velocity components were

$$\begin{aligned} v_r &= r\Omega F(\zeta) \\ v_\theta &= r\Omega G(\zeta) \\ v_z &= \frac{\sqrt{\Omega\mu_o\rho_o}}{\rho} \mathcal{H}(\zeta) \end{aligned} \tag{B-2}$$

where ζ and $\mathcal{H}$ are related to ξ and H by

$$\xi = \sqrt{\frac{\mu_o\rho_o}{\nu_\infty}} \int_o^\zeta \frac{d\zeta}{\rho} \tag{B-3}$$

and

$$H = \sqrt{\frac{\mu_o\rho_o}{\nu_\infty}} \frac{\mathcal{H}}{\rho} \tag{B-4}$$

Based on the definition of Equations (B-1) and (B-2) the dimensionless equations of motion and continuity to be solved with the computer were (cf. Equations (2-14) and (2-15))

$$\begin{aligned} F^2 - G^2 + \mathcal{H}F' &= \frac{d}{d\zeta}\left(\frac{\rho\,\mu}{\rho_o\mu_o} F'\right) \\ 2FG + \mathcal{H}G' &= \frac{d}{d\zeta}\left(\frac{\rho\mu}{\rho\,\mu} G'\right) \end{aligned} \tag{B-5}$$

$$2F + \mathcal{H}' = 0 \tag{B-6}$$

where primes refer to differentiation with respect to ζ. The dimensionless equation of convection diffusion becomes (cf. Equation (2-22))

$$\left(\mathcal{H} + \mathcal{J}\,\frac{dt_+}{d\omega_s}\right)\frac{d\omega_s}{d\zeta} = \frac{d}{d\zeta}\left(\frac{D\rho^2}{\mu_o\rho_o}\,\frac{d\omega_s}{d\zeta}\right). \tag{B-7}$$

The dimensionless current was defined as

$$\mathcal{J} = \frac{M_s\, i_z}{z_+ \nu_+ F \sqrt{\Omega\mu_o\rho_o}}\,. \tag{B-8}$$

It is related to I by

$$I = \sqrt{\frac{\mu_o\rho_o}{\nu_\infty}}\,\frac{1}{\rho_\infty}\,\mathcal{J}. \tag{B-9}$$

The boundary conditions in terms of these dimensionless quantities are at $\zeta = 0$, $F = 0$, $G = 1$, $\mathcal{H} = \dfrac{\nu_+ M_+ \mathcal{J}}{M_s}$

$$\omega_s = \omega_{zero}$$

$$-\frac{D\rho^2}{\mu_o\rho_o}\,\frac{d\omega_s}{d\zeta} = \mathcal{J}\,\omega_s t_-$$

at $\zeta = \infty$, $F = 0$ $G = 0$, $\omega_s = \omega_\infty$.

For the concentration polarization, the equation corresponding to Equation (5-4) becomes

$$\frac{F\phi_c(0)}{RT} - \frac{z_+\nu_+F^2\mu_o\rho_o\mathcal{J}}{RT\,M_s}\int_0^\infty\left(\frac{1}{\kappa} - \frac{1}{\kappa_\infty}\right)\frac{d\zeta}{\rho} + \frac{(\nu_+ + \nu_-)}{z_+\,\nu_+}\int_{(\gamma m)_o}^{(\gamma m)_\infty}(t_+ - 1)\,\frac{d\gamma m}{\gamma m}\,.$$

The program was written in FORTRAN II; it consisted of the main program DISK and three subroutines FLUID, CALC, and INFSC.

DISK is the overall control program. It read the input data and wrote the output. It calculated the concentration polarization and converted the old definitions of dimensionless quantities ζ, $\mathcal{H}$ and

```
*       LABEL
*       DECKS
*       FORTRAN
        FUNCTION CAPPA(W)
        CAPPA=0.2179*W**0.78957
        RETURN
        END
*       LABEL
*       DECKS
*       FORTRAN
        FUNCTION RHO(W)
        RHO = 0.99669+0.026901*W**0.5+0.74771*W+0.80718*W**1.5
        RETURN
        END
*       LABEL
*       DECKS
*       FORTRAN
        FUNCTION TM (W)
        TM = 0.597063+3.57889*W-8.21995*W**1.5
        RETURN
        END
*       LABEL
*       DECKS
*       FORTRAN
        FUNCTION TP(W)
        TP= -3.57889+12.329925*W**0.5
        RETURN
        END
*       LABEL
*       DECKS
*       FORTRAN
        FUNCTION S(W)
        DM=0.207*EXPF(-29.0*W**0.5)+0.638-0.580*W**0.5
        RHO =0.9967 +0.0269*W**0.5+0.7477*W+0.8072*W**1.5
        S=DM*RHO**2/(0.8937*0.99708)/10.**3
        RETURN
        END
*       LABEL
*       DECKS
*       FORTRAN
        FUNCTION VIS(W)
        RH  = 0.9967+0.0269*W**0.5+0.7477*W+0.8072*W**1.5
        U=0.88865+0.33675*W**0.5+11.3382*W**1.5+4.99107*W**2
        VIS =RH /0.99708*U/0.8937
        RETURN
        END
*       LABEL
*       DECKS
*       FORTRAN
        FUNCTION VISP(W)
        VISP=(.17977/W**0.5+0.6735+18.4048*W**0.5+11.10284*W+21.52958*W**1
      1 .5+38.65205*W**2+14.10078*W**2.5)/(0.8937*0.99708)
        RETURN
        END

*       DECKS
*       FORTRAN
        FUNCTION CONC(W)
        CONC= -0.59706*LOGE(W)+9.4576*W**0.5-24.8455*W+43.3931*W**1.5
     $  -96.5876*W**2+185.5056*W**2.5-132.2938*W**3+2.34855*W**3.5
```

```
     $ -0.89472*W**4.0+1.82266*W**4.5
       RETURN
       END

*      LABEL
*      DECKS
*      FORTRAN
       SUBROUTINE CALC
       DIMENSION F(1001),G(1001),H(1001),W(1001),V(1001),VP(1001),B(1001),
     1 ,DUM(5005)
       COMMON WINF,N,NM1,DY,AMP,GNUP,TMO,VINF,HINF,W,F,G,H,V,VP,B,DUM,
     $ WZERO
       TPINF= TP(WINF)
       W(1)= 0.0
       B(1)= 0.0
       S1= S(WZERO)
       ADD1= (AMP*TP(WZERO) + H(1))/S1
       DO 3 J=2,N
       S2= S(W(J))
       ADD2= (AMP*TP(W(J)) + H(J))/S2
       B(J)= B(J-1) + DY/2.0*(ADD1 + ADD2)
       W(J)= W(J-1) + DY/2.0*(EXPF(B(J))/S2 + EXPF(B(J-1))/S1)
       ADD1= ADD2
    3  S1= S2
       CONST=(WINF-WZERO)/(W(N)-EXPF(B(N))/(AMP*TPINF + HINF))
       DO 4 J=1,N
    4  W(J)= CONST*W(J) + WZERO
       AMP= - CONST/TMO/(1.0-WZERO)
       H(1)= GNUP*AMP
       V(1)=VIS(W(1))
       VP(1)=VISP(W(1))/CONST/S(W(1))
       NP=N-1
       DO 5 J=2,NP
       V(J)=VIS(W(J))
    5  VP(J)=VISP(W(J))*(W(J+1)-W(J-1))/(2.*DY)
       V(N)=VIS(W(N))
       VP(N)=VISP(W(N))*(W(N)-W(N-1))/DY
       RETURN
       END

*      LABEL
*      DECKS
*      FORTRAN
       SUBROUTINE INFSC
C      SUBROUTINE FOR OBTAINING THE FIRST TERMS OF THE INNER EXPANSIONS
C      OF THE VELOCITIES FOR HIGH SCHMIDT NUMBERS FOR A ROTATING DISK
C      WITH ACCOUNT BEING TAKEN OF PROPERTY VARIATIONS AND A FINITE
C      INTERFACIAL VELOCITY
       DIMENSION F(1001),G(1001),H(1001),W(1001),V(1001)
       COMMON WINF,N,NM1,DY,AMP,GNUP,TMO,VINF,HINF,W,F,G,H,V
       CONST= 0.51023*DY/2.0*SQRTF(VINF)
       F(1)= 0.0
       G(1)= 1.0
       DO 1 J=2,N
       G(J)= 1.0
       F(J)= F(J-1) + CONST/V(J) + CONST/V(J-1)
    1  H(J)= H(J-1) - DY*(F(J) + F(J-1))
       RETURN
       END
```

```
*       LABEL
*       SYMBOL TABLE
*       DECKS
*       FORTRAN
        SUBROUTINE FLUID
        DIMENSION F(1001),G(1001),H(1001),W(1001),V(1001),VP(1001),FF(1001
      1 ),FG(1001),GF(1001),GG(1001),HF(1001),HG(1001)
        COMMON WINF,N,NM1,DY,AMP,GNUP,TMO,VINF,HINF,W,F,G,H,V,VP,
      1 FF,FG,GF,GG,HF,HG
        GPS= 0.5/DY*(G(3) - G(1))
        FPS= 0.5/DY*(F(3) - F(1))
        GG(1)= 0.0
        GF(1)= 0.0
        FG(1)= 0.0
        FF(1)= 0.0
        HF(1)= 0.0
        HG(1)= 0.0
        DO 1 J=2,NM1
        GP= GPS
        FP= FPS
        GPS= 0.5/DY*(G(J+2) - G(J))
        FPS= 0.5/DY*(F(J+2) - F(J))
        H1= DY + DY*FF(J-1) - HF(J-1)
        H2= DY*FG(J-1) - HG(J-1)
        A= (V(J)/DY - 0.5*(VP(J) - H(J)))/DY
        C1= - 2.0*(V(J)/DY/DY + F(J)) + A*GG(J-1) + H2*GP
        C2= - 2.0*G(J) + A*GF(J-1) + H1*GP
        R= - (V(J)/DY + 0.5*(VP(J) - H(J)))/DY
        RG=GP*(H(J-1)-DY*F(J-1)-H(J)) - 2.0*F(J)*G(J) - A*G(J-1)
        C3= 2.0*G(J) + A*FG(J-1) + H2*FP
        C4= - 2.0*(V(J)/DY/DY + F(J))+A*FF(J-1) + H1*FP
        RF= FP*(H(J-1)-DY*F(J-1)-H(J)) - F(J)*F(J) + G(J)*G(J) - A*F(J-1)
        DET= C1*C4 - C3*C2
        FG(J)= - C3*R/DET
        GG(J)=   C4*R/DET
        FF(J)=   C1*R/DET
        GF(J)= - C2*R/DET
        F(J)= (C1*RF - C3*RG)/DET
        G(J)= (C4*RG - C2*RF)/DET
        HF(J)= - H1*FF(J) - H2*GF(J)
        HG(J)= - H1*FG(J) - H2*GG(J)
      1 H(J)= H(J-1) - H1*F(J) - H2*G(J) - DY*F(J-1)
        DO 3 K=1,10
        C3= 2.0*VINF/HINF
        C1= (C3-DY)/(C3+DY) - GG(NM1)
        C2= (C3-DY)/(C3+DY) - FF(NM1)
        DET= C1*C2 - GF(NM1)*FG(NM1)
        F(N)= (FG(NM1)*G(NM1) + C1*F(NM1))/DET
        G(N)= (GF(NM1)*F(NM1) + C2*G(NM1))/DET
      3 HINF= H(NM1) + C3*F(NM1)+(HG(NM1)+C3*FG(NM1))*G(N) +(HF(N-1)+C3*
      1 FF(NM1))*F(N)
        H(N)= HINF - C3*F(N)
        DO 2 K=2,NM1
        J= N - K + 1
        G(J)= G(J) + GG(J)*G(J+1) + GF(J)*F(J+1)
        F(J)= F(J) + FG(J)*G(J+1) + FF(J)*F(J+1)
      2 H(J)= H(J) + HG(J)*G(J+1) + HF(J)*F(J+1)
        RETURN
        END
```

```
*       LABEL
*       SYMBOL TABLE
*       DECKS
*       FORTRAN
C2DIS K
C       PROGRAM FOR MASS TRANSFER TO ROTATING DISK, BINARY SOLUTION
        DIMENSION F(1001),G(1001),H(1001),W(1001),V(1001),DUM(7007)
        COMMON WINF,N,NM1,DY,AMP,GNUP,TMO,VINF,HINF,W,F,G,H,V,DUM,WZERO
  101   FORMAT (//  12X, 35H INFINITE SCHMIDT NUMBER IS ASSUMED)
  102   FORMAT (I5,1P4E14.4)
  103   FORMAT (5E8.4,4X,5I4)
  104   FORMAT (55H1                          AMP        WINF     DY     GNUP      TMO
      1 /13X,E13.4,2F7.3,2F8.4//49H0  HINF      RAB          KW            RV
      2         GPO/2F9.5, 2E12.4, F9.5//56H0    J          W              F
      3            G              H/(I5,1P4E14.4))
  105   FORMAT (32H0 CONCENTRATION OVERPOTENTIAL IS, 1PE14.4,  6H  PLUS, 1
      1 PE14.4/ 7H WZERO=, 1PE16.6)
  106   FORMAT (1H  //)
  107   FORMAT (1H1,8X, 24H DIMENSIONLESS CURRENT =, E12.4 /
      $  8X, 17H HH AT INFINITY =, E12.4/   73H0  J          XI              W
      $              F              G              HH          )
  108   FORMAT (I5, 1P5E14.4)
        HINF= - 0.884
        READ INPUT TAPE 2,103, DY
        N= 201
        NM1= 200
        DO 6 J=1,N
        V(J)= 1.0
    6   G(J)= 0.005*FLOATF(N-J)
        DO 7 J=1,5
    7   CALL FLUID
    1   READ INPUT TAPE 2,103,WINF,WZERO,ERR,GNUP,CONST,N,M,NS,INF,NO
        VINF= VIS(WINF)
        TMO = TM(WZERO)
        NM1= N - 1
        DO 2 J=1,N
    2   W(J)= 0.0
        AMP= 0.0
    3   AO= AMP
        HNO= HINF
        CALL CALC
        GO TO (11,12),INF
   11   CALL FLUID
        GO TO 13
   12   CALL INFSC
   13   IF (ABSF(HINF - HNO) - ERR)  4,4,3
    4   IF (ABSF(AMP - AO) - ERR*ABSF(AMP))  5,5,3
    5   GPO= (G(2) - G(1))/DY/(1.0+0.5*DY*H(1))
        RAB= - GNUP*(WINF-WZERO)/TMO/(1.0-WZERO)
        AKW= - TMO*AMP/(WINF-WZERO)*(1.0-WZERO)
        RV= 0.0
        GO TO (14,15),INF
   14   RV= - H(1)/GPO
   15   WRITE OUTPUT TAPE 3,104,    AMP,WINF,DY,GNUP,TMO,HINF,RAB,AKW,RV,
      1 GPO,(J,W(J),F(J),G(J),H(J),J=1,10)
        GO TO (8,9),NO
    8   GO TO (17,16),INF
   16   WRITE OUTPUT TAPE 3,101
```

```
17    WRITE OUTPUT TAPE 3,106
      WRITE OUTPUT TAPE 3,102, (J,W(J),F(J),G(J),H(J),J=1,NS,M)
 9    IF (W(1)) 1,1,18
18    ETAC1=0.0
      CAPINF=CAPPA(WINF)
      DO 24 J=1,10
      CAPPA1=CAPPA(W(J))*RHO(W(J))
      CAPPA2=CAPPA(W(J+1))*RHO(W(J+1))
24    ETAC1=ETAC1+DY*(1.0/(CAPPA2-CAPPA1)*LOGF(CAPPA2/CAPPA1)-1.0/CAPINF
    $ *(0.5/RHO(W(J))+0.5/RHO(W(J+1))))
      DO 19 J=12,N
19    ETAC1=ETAC1+DY*(0.5/CAPPA(W(J-1))/RHO(W(J-1))+0.5/CAPPA(W(J))/RHO(
    $ W(J))-1.0/CAPINF*(0.5/RHO(W(J-1))+0.5/RHO(W(J))))
      ETAC1= CONST*AMP*ETAC1
      ETAC2= CONC(WINF)-CONC(W(1))
      WRITE OUTPUT TAPE 3,105, ETAC1,ETAC2,WZERO
      SUM=0.0
      XI=0.0
      RINF=RHO(WINF)
      COEFF=RINF*1.0/SQRTF(VINF)
      CURREN=1.0/SQRTF(VINF)*AMP
      HHINF=1.0/SQRTF(VINF)*HINF
      WRITE OUTPUT TAPE 3,107, CURREN,HHINF
      DO 22 J=1,NS
      HH=COEFF/RHO(W(J))*H(J)
      IF (J-1) 21,21,20
20    SUM=SUM+DY*(0.5/RHO(W(J-1))+0.5/RHO(W(J)))
      XI=COEFF*SUM
      IF (J-41) 21,21,23
23    MM=(J-1)/M
      JJ=MM*M+1
      IF (J-JJ) 22,21,22
21    WRITE OUTPUT TAPE 3,108, (J,XI,W(J),F(J),G(J),HH)
22    CONTINUE
      GO TO 1
      END
```

$\mathcal{L}$ to the definitions used in this paper, ξ, H and I by Equations (B-3), (B-4) and (B-9), respectively.

FLUID is the subroutine which carries out the numerical solution of the three velocity components F, G and $\mathcal{H}$ at each mesh point. The detailed numerical method has been given in section 2-4.

INFSC is the subroutine for calculating the velocity components F, G, and H by a singular perturbation method when an infinite Schmidt number is assumed.

CALC handles the concentration profile by solving Equation (B-7).

Eight functional programs were designed for evaluating the physical properties and other necessary dimensionless groups of copper sulfate solution at 25°C, they are

1. CAPPA $= \kappa$
2. RHO $= \rho$
3. TM $= t_-$
4. TP $= \dfrac{dt_+}{d\omega}$
5. S $= \dfrac{D\rho^2}{\mu_o \rho_o}$
6. VIS $= \dfrac{\rho\,\mu}{\rho_o \mu_o}$
7. VISP $= \dfrac{d}{d\omega}\left(\dfrac{\rho\mu}{\rho_o \mu_o}\right)$
8. CONC $= \displaystyle\int_{(\gamma m)_o}^{(\gamma m)_\infty} (t_+^o - 1)\,\frac{d\gamma m}{\gamma m}$

Two data cards are required, they are

<u>Card I</u>

DY is mesh size used in solving the linearized ordinary differential

equations. The total mesh number is 1001, the mesh size should not be smaller than 0.01 in order to have an accurate calculation of the fluid velocity. Otherwise the range of ζ covered will not include enough of the hydrodynamic boundary layer.

Card II

1. WINF is bulk concentration of solution in terms of mass fraction.
2. WZERO is the concentration at interface in terms of mass fraction.
3. ERR is error tolerance in calculating normal component velocity H. 10^{-5} is recommended for this program.
4. GNUP is $\frac{\nu_+ M_+}{M_s}$.
5. CONST is $\frac{z_+ \nu_+ F^2 \mu_o \rho_o}{RT\, M_s}$.
6. N is total number of mesh points to be used. The maximum storage is 1001.
7. M is the interval of mesh points to be printed out.
8. NS is the number of mesh points to be printed out.
9. INF is a selector.

   INF = 1 subroutine FLUID being used for calculating velocity profile.

   INF = 2 subroutine INFSC being used.
10. NO is output selector.

    NO = 1 program printed out mesh number, ω_s, F, G, H.

    NO = 2 program printed out mesh number, ξ, ω_s, F, G, H.

NOMENCLATURE

C - concentration of binary electrolyte.

C_i - concentration of species i (moles/cm^3).

d - diameter of disk.

d_o - diameter of disk electrode.

D - molecular diffusion coefficient of binary electrolyte.

e^- - symbol for electron.

F - radial dimensionless velocity component (2-11).

F - Faraday's constant (coulomb/equiv).

G - tangential dimensionless velocity component (2-11).

h - mesh size for numerical solution of differential equation.

H - normal dimensionless velocity component (2-11).

$\mathcal{H}$ - normal dimensionless velocity component (B-2).

g - acceleration of gravity (cm/sec^2).

$\underline{i}$ - current density (amp/cm^2).

i_o - exchange current density (amp/cm^2).

I - dimensionless current density.

$\mathcal{J}$ - dimensionless current density.

m - molality.

M_i - molecular weight of species i.

M_s - molecular weight of salt.

n - number of electrons in equation for electrode reaction.

$\underline{N}_i$ - molar flux of species i (moles/cm^2-sec).

n_i - mass flux of species i (g/cm^2-sec).

p - pressure (dyne/cm^2).

P - dimensionless pressure.

Q_i - symbol for the chemical formula of species i.

r - radius of disk.

r_o - radius of disk electrode.

R - universal gas constant.

R - total resistance of solution.

$R' - \frac{d \ln \rho}{d\xi}$.

S_i - stoichiometric coefficient in equation for electrode reaction.

Sc - Schmidt number $Sc = \frac{\nu}{D}$.

t_i - transference number with respect to mass average velocity at species i.

$U' - \frac{\rho_\infty}{\rho} \frac{d}{d\xi} \left(\frac{\mu}{\mu_\infty}\right)$.

v - (mass average) fluid velocity (cm/sec)

$V - \frac{\mu}{\mu_\infty} \frac{\rho_\infty}{\rho}$.

z_i - valence or charge number of species i.

α - transfer coefficient in polarization equation.

γ - mean molal activity coefficient.

δ_{ij} - the Kronecker delta

$$\delta_{ij} = 1 \text{ if } i = j$$
$$\delta_{ij} = 0 \text{ if } i \neq j.$$

ϵ_D - diffusivity perturbation parameter.

ϵ_ρ - density perturbation parameter.

ζ - dimensionless distance (B-1).

κ - specific conductivity $ohm^{-1}cm^{-1}$.

λ_o - dimensionless distance between reference electrode and rotating disk electrode.

μ_e - chemical potential of salt in binary electrolyte.

ν - kinematic viscosity (cm^2/sec).

ν_+, ν_- - number of cations and anions produced by dissociation of one molecule of electrolyte.

ξ - dimensionless distance from the rotating disk (2-10).

ρ - density of solution.

$\underline{\underline{\tau}}$ - stress tensor (2-2).

ϕ_a - activation (chemical) overpotential.

ϕ_c - concentration (diffusion) overpotential.

ϕ_{ohm} - ohmic resistance overpotential.

ω_s - mass fraction of salt in binary electrolyte.

Ω - rotating speed of disk electrode (radians/sec).

Subscripts

+,-,o - cation, anion, and solvent in binary electrolyte.

∞ - in the bulk of solution.

s - salt.

lim - denotes limiting current.

zero - at the interface of electrode and solution.

LITERATURE CITED

1. Veniamin G. Levich. "The Theory of Concentration Polarization." Acta Physicochimica U.R.S.S., 17, 257-307 (1942).

2. Veniamin G. Levich. Physicochemical Hydrodynamics. Englewood Cliff: Prentice-Hall, Inc., 1962. a-pp. 286-293.

3. A. C. Riddiford. "The Rotating Disk System." Advances in Electrochemistry and Electrochemical Engineering, Vol. 5; P. Delahay and C. W. Tobias, eds. New York: Interscience Publishers, in preparation.

4. D. R. Olander. "Unsteady-state Heat and Mass Transfer in the Rotating Disk Revolving Fluid System." International Journal of Heat and Mass Transfer, 5, 825-836 (1962).

5. J. M. Hale. "Theory of Galvanonstatic and Galvanostatic with Current Reversal Transients at a Rotating Disk Electrode." Journal of Electroanalytical Chemistry, 6, 187-197 (1963).

6. V. Y. Filinovskii and V. A. Kiryanov. "Contribution of the Theory of Nonstationary Convective Diffusion Near a Rotating Disk Electrode." Proceedings of the Academy of Sciences of the USSR, 156, 650-653 (1964).

7. John S. Newman and L. Hsueh. "The Effect of Variable Transport Properties on Mass Transfer to a Rotating Disk." UCRL-16623, February 1966.

8. O. R. Brown and H. R. Thirsk. "The Rate-Determining Step in the Electrodeposition of Copper in Copper from Aqueous Cupric Sulfate Solutions." Electrochimica Acta, 10, 383-393 (1965).

9. D. R. Olander. "The Influence of Physical Property Variations on Liquid-Phase Mass Transfer for Various Laminar Flows." International Journal of Heat and Mass Transfer, 5, 765-780 (1962).

10. R. B. Bird, W. E. Stewart, and E. N. Lightfoot. Transport Phenomena. New York: John Wiley & Sons, Inc., 1960. a-p. 85 b-p. 89.

11. Th. v. Karman. "Uber laminare und turbulente Reibung." Zeitschrift für angewandte Mathematik und Mechanik, 1, 233-252 (1921).

12. John S. Newman. "Transport Processes in Electrolytic Solutions." To be published in Advances in Electrochemistry and Electrochemical Engineering.

13. W. G. Cochran. "The Flow Due to a Rotating Disc." Proceedings of the Cambridge Philosophical Society, 30, 365-375 (1934).

14. Klaus J. Vetter. Elektrochemische Kinetik. Berlin: Springer-Verlag, 1961.

15. R. Parsons. "General Equations for the Kinetics of Electrode Processes." Transactions Faraday Society, 47, 1332-1344 (1951).

16. J. V. Petrocelli. "The Kinetics of Oxidation-Reduction Electrode Reactions." Journal of the Electrochemical Society, 98, 187-192 (1951).

17. N. Tanaka and R. Tamamushi. "Kinetic Parameters of Electrode Reaction." Electrochimica Acta, 9, 963-989 (1964).

18. C. Kasper. "The Theory of the Potential and the Technical Practice of Electrodeposition. I-II." Transactions Electrochemistry Society, 77, 353-384 (1940).

19. D. Jahn and W. Vielstich. "Rates of Electrode Processes by the Rotating Disk Method." Journal of the Electrochemical Society, 109, 849-852 (1962).

20. G. R. Johnson and D. R. Turner. "The Effect of Some Addition Agents on the Kinetics of Copper Electrodeposition from a Sulfate Solution." "II. Rotating Disk Electrodes Experiments." Journal of the Electrochemical Society, 109, 918-922 (1962).

21. Z. Galus and Ralph N. Adams. "The Investigation of the Kinetics of Moderately Rapid Electrode Reactions Using Rotating Disk Electrodes." Journal of Physical Chemistry, 67, 866-871 (1963).

22. John S. Newman. "Resistance for Flow of Current to a Disk." UCRL-16498. November (1965).

23. T. Theodorsen and A. Regier. "Experiments on Drag of Revolving Disk, Cylinders and Streamlines Rods at High Speed." National Advisory Committee for Aeronautics, No. 793, 367-384 (1944).

24. N. Ibl and K. Schadegg. "Study of the Electrodeposition of Copper in the Limiting Current Range." To be published.

25. V. A. Belyaeva. "A New Design of the Rotating Disk Electrode." Russian Journal of Physical Chemistry, 36, 743-744 (1962).

26. Hermann Schlichting. Boundary Layer Theory. New York: McGraw-Hill Book Company, Inc., 1960. Chapter 20-21.

27. Seward E. Beacom and R. N. Hollyer, Jr. "Rotating Disk Electrode Techniques for the Study of Addition Agents." "I. Preliminary Studies with Cupric Sulfate Solutions." Journal of the Electrochemical Society, 109, 495-497 (1962).

28. G. T. Rogers and K. J. Taylor. "Effect of Small Protrusions on Mass Transfer to a Rotating Disk Electrode." Nature, 200, 1062-1064 (1963).

29. L. Karasyk and H. B. Lindford. "Electrode Kinetic Parameters for Copper Deposition on Clean and Soiled Copper Cathodes." Journal of the Electrochemical Society, 110, 895-903 (1963).

30. D. P. Gregory and A. C. Riddiford. "Transport to the Surface of a Rotating Disc." Journal of Chemical Society, 3756-3764 (1956).

31. John S. Newman. "Schmidt Number Correction for the Rotating Disk." Submitted for publication.

32. J. J. Fritz and C. R. Fuget. "Measurement of the Transference Number of Aqueous Copper Sulfate Solution by the Moving Boundary Method." Journal of Physical Chemistry, 62, 303-305 (1958).

33. W. G. Eversole, H. M. Kindswater and J. D. Peterson. "The Molar at 25°C." Journal of Physical Chemistry, 46, 370-375 (1942).

34. A. Emanuel and D. R. Olander. "Diffusion Coefficients of Copper Sulfate in Water and Water in n-Butyl Alcohol." Journal of Chemical and Engineering Data 8, 31-32 (1963).

35. J. N. Pearce and G. G. Pumplin. "The Apparent and Partial Molal Volumes of Ammonium Chloride and Cupric Sulfate in Aqueous Solution at 25°C." Journal of the American Chemical Society, 59, 1221-1222 (1937).

36. E. Asmus. "Über die Zähigkeit wäbriger Lösungen starker Elektrolyte Löheren Valenztyps." Annalen der Physik, Ser. 5, 35, 1-22 (1939).

37. H. D. Holler and E. L. Pepper. "The Density of Aqueous Solutions of Copper Sulfate and Sulfuric Acid." Journal of the American Chemical Society, 38, 1021-1029 (1916).

38. B. B. Owen and R. W. Gurry. "The Electrolytic Conductivity of Zinc Sulfate and Copper Sulfate in Water at 25°C." Journal of the American Chemical Society, 60, 3074-3078 (1938).

39. H. K. Richardson and F. D. Tayler. "The Conductivity of Mixtures of Copper Sulfate and Sulfuric Acid." Transactions of the American Electrochemical Society, 20, 179-184 (1911).

40. B. Fedoroff. "Contribution a l'étude des sulfates simples et doubles de quelques métaux de la série magnésienne." Annales de Chimie, Ser. 11, 16, 154-214 (1941).

41. R. F. Nielsen and D. J. Brown. "The Potential of a Proposed Standard Form of Copper and the Activity of Copper Sulfate." Journal of the American Chemical Society, 49, 2423-2438 (1927).

42. R. A. Robinson and R. S. Jones. "The Activity Coefficients of Some Bivalent Metal Sulfates in Aqueous Solution from Vapor Pressure Measurements." Journal of the American Chemical Society, 58, 959-961 (1936).

43. F. E. W. Wetmore and A. R. Gordon. "The Activity Coefficient of Copper Sulfate in Aqueous Solution." Journal of Chemical Physics, 5, 60-63 (1937).

44. R. A. Robinson and R. H. Stokes. "Tables of Osmotic and Activity Coefficient of Electrolytes in Aqueous Solution at 25°." Transaction of the Faraday Society, 45, 612-624 (1949).

45. E. Asmus. "Die Zähigkeit von Gemischen wäbriger Lösungen starker Electrolyte mit besonderer Berücksichtigung der Theorie von Onsager und Fuoss." Annalen der Physik. Ser. 5, 36, 166-182 (1938).

46. E. Asmus. "Versuche zur Falkenhagenschen Theorie der Zähigkeit verdünnter wässeriger Lösungen starker Elektrolyte." Zeitschrift für Physik 108, 491-499 (1938).

47. W. Herz, "Die innere Reibung von Salzlösungen." Zeitschrift für Anorganische Chemie, 89, 393-396 (1914).

This report was prepared as an account of Government sponsored work. Neither the United States, nor the Commission, nor any person acting on behalf of the Commission:

A. Makes any warranty or representation, expressed or implied, with respect to the accuracy, completeness, or usefulness of the information contained in this report, or that the use of any information, apparatus, method, or process disclosed in this report may not infringe privately owned rights; or

B. Assumes any liabilities with respect to the use of, or for damages resulting from the use of any information, apparatus, method, or process disclosed in this report.

As used in the above, "person acting on behalf of the Commission" includes any employee or contractor of the Commission, or employee of such contractor, to the extent that such employee or contractor of the Commission, or employee of such contractor prepares, disseminates, or provides access to, any information pursuant to his employment or contract with the Commission, or his employment with such contractor.